The Thesis Committee for Dustin Donald Holden
Certifies that this is the approved version of the following thesis:

Hybrid Activation for Intact Protein and Peptide Characterization

APPROVED BY
SUPERVISING COMMITTEE:

Supervisor:

Jennifer S. Brodbelt

Charles B. Mullins

Hybrid Activation for Intact Protein and Peptide Characterization

by

Dustin Donald Holden, B.S. Bioch.

Thesis

Presented to the Faculty of the Graduate School of

The University of Texas at Austin

in Partial Fulfillment

of the Requirements

for the Degree of

Master of Arts

The University of Texas at Austin

May 2015

Abstract

Hybrid Activation for Intact Protein and Peptide Characterization

Dustin Donald Holden, M.A.

The University of Texas at Austin, 2015

Supervisor: Jennifer S. Brodbelt

Mass spectrometers may be utilized to generate and detect fragmentation patterns of peptides and proteins to acquire mass spectra that allow for accurate amino acid sequence characterization and localization of post-translational modifications. Conventional activation methods utilize collisions with neutral gas molecules to collisionally activate these ions but have some drawbacks, being dependent on charge state and amino acid sequence characteristics. More recent activation methods include radical transfer as well as ultraviolet photodissociation, the latter of which impart higher energy into target ions providing more extensive fragmentation patterns and more sequence information. In the following research all of these activation methods were explored with peptide and protein cations as well as various combinations of such methods to investigate their benefits and limitations. In summary, ultraviolet photodissociation provides the most diverse fragmentation patterns of all researched. Combining radical transfer and subsequent ultraviolet photodissociation termed "hybrid activation" generated interesting effects such as spectral simplification as well as

constructive inclusion of fragment ions lacking in ultraviolet photodissociation. Included in this thesis are those interesting findings.

Table of Contents

Chapter One: Hybridizing Ultraviolet Photodissociation with Electron Transfer Dissociation for Intact Protein Characterization[1]

OUTLINE 1.1

We report a hybrid fragmentation method involving electron transfer dissociation (ETD) combined with ultraviolet photodissociation (UVPD) at 193 nm for analysis of intact proteins in an Orbitrap mass spectrometer. Integrating the two fragmentation methods resulted in an increase in the number of identified c- and z-type ions observed when compared to UVPD or ETD alone, as well as generating a more balanced distribution of a/x, b/y and c/z ion types. Additionally, the method was shown to decrease spectral congestion via fragmentation of multiple (charge-reduced) precursors. This hybrid activation method was facilitated by performing both ETD and UVPD within the HCD cell of the Orbitrap mass spectrometer which allowed a greater than two-fold reduction in duty cycle and concomitant increase in the total number of fragment ions in comparison to the analogous MS^3 format in which ETD and UVPD were undertaken in separate segments of the mass spectrometer. The feasibility of the hybrid method for characterization of proteins on a liquid chromatography timescale characterization was demonstrated for intact ribosomal proteins.

INTRODUCTION 1.2

Electron capture dissociation and electron transfer dissociation (ECD and ETD, respectively)[1,2] have become landmark ion activation/dissociation methods in the field of proteomics due to their ability to maintain labile post translational modifications (PTMs) while indiscriminately fragmenting the polypeptide backbone. Both ECD and ETD

[1] Cannon, Joe R., Dustin D. Holden, and Jennifer S. Brodbelt. 2014. "Hybridizing Ultraviolet Photodissociation with Electron Transfer Dissociation for Intact Protein Characterization." *Analytical Chemistry* 86 (21): 10970–77. doi:10.1021/ac5036082. (J.R. Cannon and D.D. Holden contributed equally to this work, J.S. Brodbelt was principal investigator)

promote similar mechanisms of ion activation and fragmentation and have been used extensively for localization of PTMs in bottom-up peptide-based analysis and in top down mass spectrometry for characterization of intact proteins.[3] A compelling feature of electron-based activation methods is the ability to generate charge-reduced ions, including ample abundances of odd electron (radical) precursors that may be isolated and further energized. In this way, the fragmentation of odd electron (radical) versus even electron (closed shell) peptides and proteins may be conveniently compared, not only shedding light on the fundamental impact of radical-mediated processes but also allowing access to a different, often complementary, type of fragmentation behavior with analytical merits (sequencing, localization of modifications, etc.). The intriguing opportunities afforded by production and analysis of radical-type ions have motivated several groups to explore hybrid methods that combine ETD with a second activation method. For example, Heck and co-workers have recently devised new approaches based on hybrid combinations of fragmentation methods for more complete peptide fragmentation.[4] In one case, electron transfer dissociation followed by transmission of all resulting ions into a multipole for higher energy collision induced dissociation (so called EThcD), was shown to provide an informative array of predominantly b-, c-, y-, and z-type ions.[4] While the greater number of fragmentation channels increased both the complexity of the product ion spectrum and the fragment ion search space for all candidate peptides that fell within the precursor mass tolerance, the net increase in information more than compensated for the decrease in confidence from a typical database search.[4] Moreover, the hybrid EThcD method improved the localization scores obtained for identification of phosphorylation sites of peptides.[5] We have evaluated the use of hybrid methods combining electron transfer reactions to generate radical cations, followed by CID, infrared multiphoton dissociation (IRMPD), or ultraviolet

photodissociation (UVPD) for characterization of the sites of modification of nucleic acids.[6] The most diverse array of fragment ions was obtained from the ETUVPD hybrid method, an outcome that proved particularly beneficial for specific localization of modifications for which fragmentation was suppressed for other activation methods.[6] We have also explored the use of UVPD to characterize radical peptide cations produced by electron transfer reactions, finding that the location of very basic sites (like Arg) at the C- versus N-terminus influenced the resulting fragmentation behavior and the preference for radical-directed versus photoactivated cleavages.[7]

Now that available bioinformatic platforms can accommodate high throughput top down MS/MS analyses that result in a multitude of ion types, such as the diverse array of fragments that arise from UVPD,[8] the potential for hybrid fragmentation of intact proteins is feasible even for complex mixtures. Recently, we have demonstrated the utility of 193 nm UVPD for intact protein characterization in both single protein infusion and high throughput type LCMS experiments.[8–10] Typically, product ion spectra following UV photoactivation are characterized by a large proportion of the total ion current residing in the surviving precursor ion and a complex distribution of fragment ions (a, b, c, x, y, z) in an array of charge states. For those proteins in higher charge states, the crowded spectra confound deconvolution algorithms and are artifactually enriched in fragment ions of low mass and lower (and more easily deconvoluted) charge.[9] This spectral complexity is the result not only of closely spaced isotopic peaks due to high charge states but also from the multitude of ion types generated by UVPD. In general, previous studies of 193 nm UVPD for top down proteomics have reported product ion spectra that have large contributions from a- and a+1-type ions representing the N terminus (with much lower proportions of b- and c-type ions), and a mixture of x-, y-, y-1-, and z-type ions arising from the C terminus.[8,10] Despite the increase in search space

associated with accommodating all of these ion types in an unweighted search algorithm, the sheer number of identified fragment ions has been shown to allow nearly complete protein characterization (via backbone cleavages present at nearly every inter-residue position).[8,10] While the number of fragment ions is very high, the method could benefit from an increase in the number and abundances of complementary C-terminally derived ions, such as the radical containing z-type ions that result from ETD, as well as a decrease in ions that are duplicative for the same inter-residue position (a and a+1, for example). The recent strategy from the Heck group for performing ETD in a DC gradient-only multipole[11] affords an opportunity to implement ETD and UVPD together in a high performance Orbitrap mass spectrometer,[8,12] as described herein. While ETUVPD can be readily implemented in an MS3 format (in which the ETD step in the LIT precedes UVPD in the HCD cell), the ability to perform ETD in the HCD cell, per the Heck concept,[11] provides more flexibility. For example, ETD can precede or follow UVPD in the HCD cell or both activation processes can be undertaken simultaneously. Ultraviolet irradiation electron transfer dissociation (UVIETD), has the potential to alleviate one of the main drawbacks of UVPD when performed by itself – a high proportion of the total ion current in the product ion spectrum resides in and/or falls very close to the m/z of the unfragmented precursor. This high peak density results in crowded spectra that are difficult to deconvolute due to their high charge states and close proximity to one another. Since ET kinetics have strong charge state dependence,[13] initiating the ETD reaction following UVPD favors the likelihood of preferential dissociation of the (more highly charged) unreacted precursor above the fragment ions also present in the cell. Here we report the analytical merits of hybridizing ETD and UVPD for top down proteomics, with emphasis on the ability to achieve a more balanced

array of product ions as well as a more uniform distribution of the ion current across the available m/z landscape.

MATERIALS AND METHODS 1.3

Model Protein Studies

Bovine ubiquitin, horse myoglobin, and bovine carbonic anhydrase were purchased from Sigma-Aldrich (St. Louis, MO) and intact ribosomes were purchased from New England Biolabs (Ipswich, MA). All other solvents and chemicals were purchased from Sigma-Aldrich. Proteins were suspended in 50/49/1 methanol/water/formic acid (v/v/v) at a final concentration of 10 μM. They were infused directly into an Orbitrap Elite mass spectrometer (Thermo Fisher Scientific, Bremen, Germany) customized for implementation of UVPD.[12] Ultraviolet irradiation was achieved via a single (unless otherwise noted) 5 ns laser pulse from a Coherent ExciStar (Santa Clara, CA) 193 nm excimer laser. Feasibility studies utilizing an MS3 mode were performed via electron transfer dissociation in either the linear ion trap (LIT) or the higher energy collision dissociation (HCD) cell, followed by UVPD of the resulting ETD product ions in the HCD cell. The *m/z* range of the ion isolation window was varied to accommodate solely the singly charge reduced radical precursor or to encompass as many of the product ions and charge-reduced precursors as possible (±300 *m/z* around the initial multi-protonated precursor). For intact protein studies ubiquitin, myoglobin, and carbonic anhydrase were reconstituted at 10 μM in 50/49/1 acetonitrile/water/formic acid (v/v/v). Spectra were acquired using 75, 200, and 500 averaged scans respectively.

ETUVPD

Custom changes to the ion trap control language (ITCL) were made to allow the ETD reaction to occur within the HCD cell and to accommodate laser triggering for ion irradiation in the HCD cell of the Orbitrap mass spectrometer.

Ribosomal LC-UVPD-MS/MS

Ribosomes were prepared as described elsewhere.[10,14,15] Briefly, intact ribosomal protein was isolated via acid precipitation of ribosomal RNA. Ribosomes were mixed with acetic acid (1 M) to a final concentration of 60% (v/v). The nucleic acids were allowed to precipitate, and the samples were centrifuged. The protein containing supernatant was reduced and alkylated. Ribosomes were analyzed using an Eksigent nanoLC Ultra system coupled to the Orbitrap Elite mass spectrometer.

Bioinformatics

Fragment ion matching for intact proteins was performed using a version of ProSightPC 3.0 (Thermo Fisher) that was customized to accommodate the fragment ion types encountered with 193 nm UVPD.[8] All product ions were matched within 10 ppm of their theoretical masses.

RESULTS AND DISCUSSION 1.4

To date UVPD has yielded extremely rich fragmentation patterns of intact proteins, yielding high sequence coverages and exceptional capabilities for pinpointing modifications albeit at the expense of sensitivity due to the greater division of ion signal into many fragment ion channels.[8–10] Optimizing the utility of the diverse fragmentation pathways for protein identification and characterization has required search algorithms to accommodate an array of fragment ion types (a, a+1, b, c, x, x+1, y, y-1, and z),[8] and with this multiplicity comes a penalty due to the concomitant increase in fragment ion search

space.[10] Despite this trade-off, the amount of information obtained using UVPD outweighs the reduction in sensitivity and expanded search space.[10] We have shown previously that the successful characterization of intact proteins such as ubiquitin, myoglobin, and carbonic anhydrase by UVPD arises in large part from the significant number of mostly a-type ions that span a high proportion of the protein backbone.[8] By combining both ETD (which results in predominantly c- and z-type ions) and UVPD, we anticipated that the ion current might be more evenly distributed, especially balancing C-terminal fragment ions with N-terminal ions. This hypothesis holds true for some proteins (e.g. myoglobin, 22+; carbonic anhydrase, 34+) but is less notable for others (ubiquitin, 13+) by ETD, UVPD and ETUVPD, as shown in **Figure 1.1** for ubiquitin and in **Figure 1.2** for myoglobin. As expected, c/z ions are more dominant in the ETD spectra, and the UVPD spectra display primarily a ions along with contributions from b, c, z, y, and z ions. The ETUVPD spectra show distributions that are intermediate between the ones observed for ETD and UVPD.

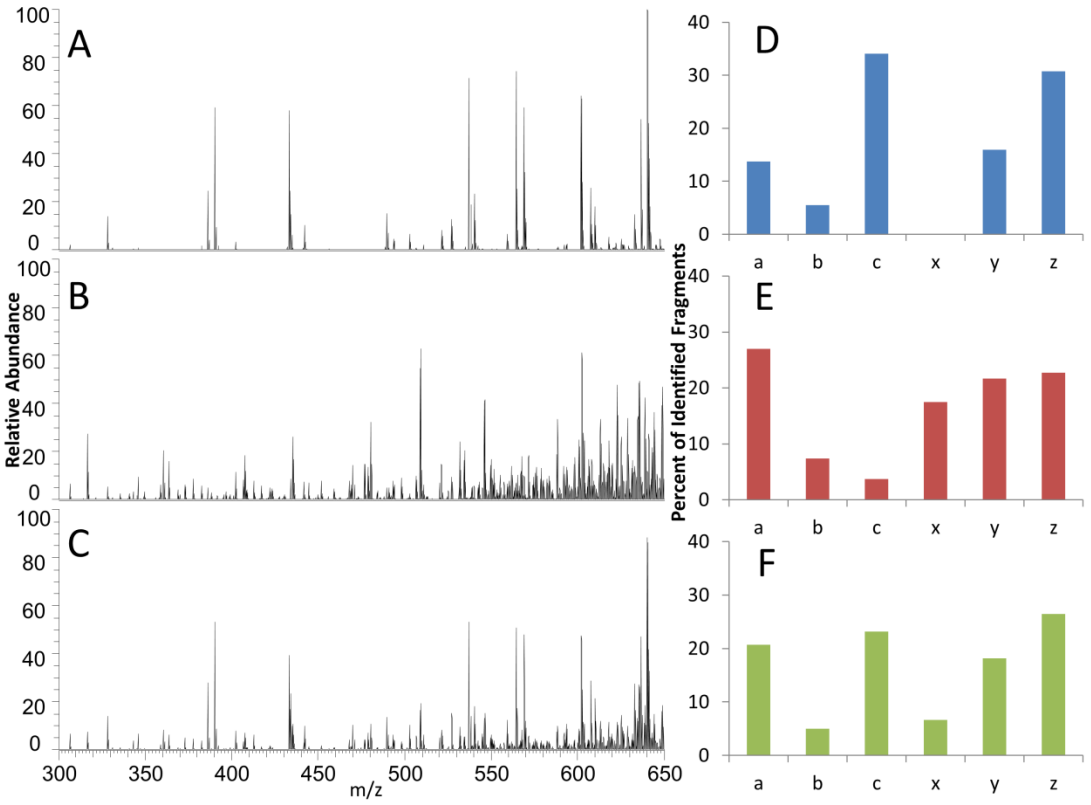

Figure 1.1. MS/MS spectra of ubiquitin (13+). A) ETD (15 ms in HCD cell), B) UVPD (one pulse, 2.5 mJ in HCD cell), C) ETUVPD (15 ms ETD in HCD cell followed by UVPD using one pulse 2.5 mJ in HCD cell) and corresponding distribution of ion types in D, E and F. All spectra are shown on the same scale.

An additional consequence of uniting ETD and UVPD is the ability to enhance the analysis of odd electron ions (such as charge-reduced precursors formed upon ETnoD and radical fragment ions initially formed upon ETD), ones that may dissociate by different, highly informative pathways and further enrich the resulting MS/MS spectra. Improved results have been reported for CID after electron transfer reactions by capitalizing on the instability of electron adducted precursors for peptide level proteomics in so-called 'charge-reduced CID' (CRCID).[16] The general idea of enhancing ETD

fragmentation by supplemental activation has been termed "activated-ion ETD",[17–20] but as of yet, there have been no studies integrating ETD and UVPD at the protein level.

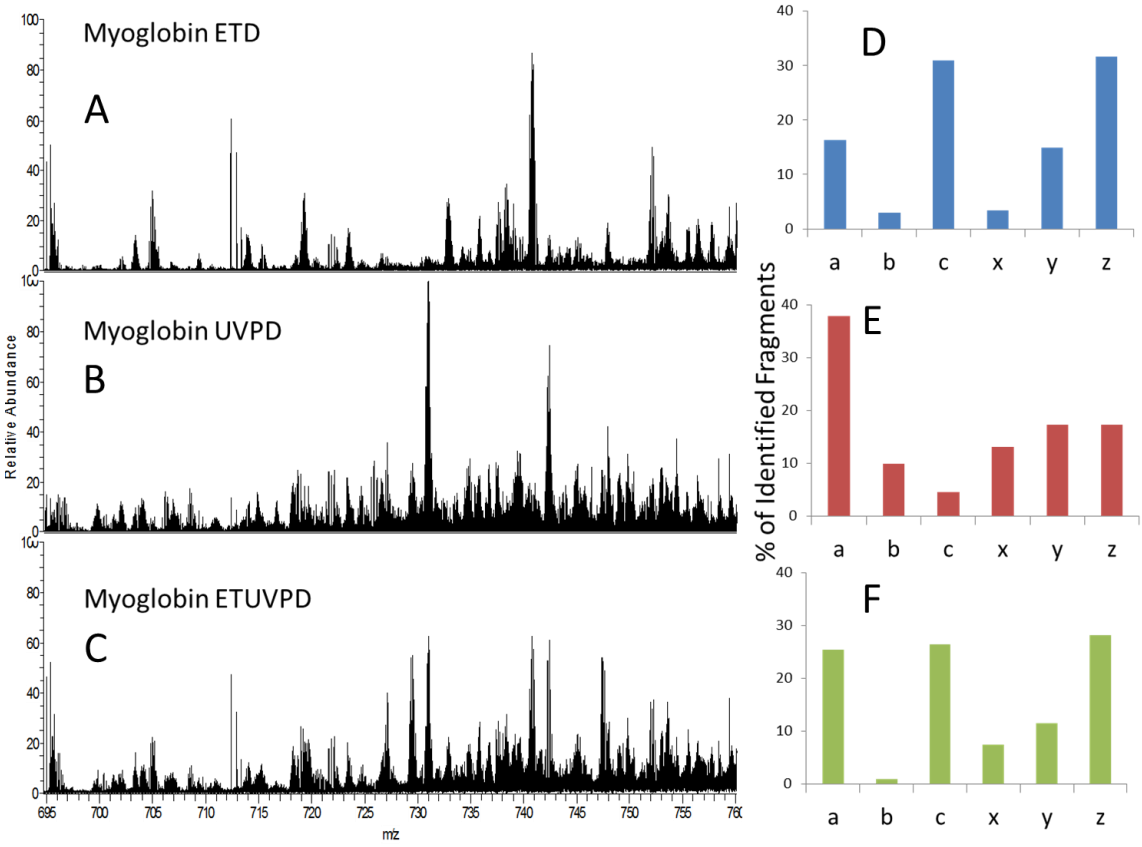

Figure 1.2. MS/MS spectra of myoglobin (22+). A) ETD (4 ms in HCD cell), B) UVPD (one pulse, 2.5 mJ in HCD cell), C) ETUVPD (4 ms ETD in HCD cell followed by UVPD using one pulse 2.5 mJ in HCD cell) and corresponding distribution of ion types in D, E and F. All spectra are shown on the same scale.

Additional feasibility experiments were conducted by comparing ETD in the linear ion trap (LIT) versus in the HCD cell prior to ultraviolet irradiation. The apparent decrease in efficiency of electron transfer from the reagent ion to the protein polycation was observed as expected[11] when the reaction was performed in the HCD cell when

compared to the reaction in the LIT. In the HCD cell, the reduced overlap between the reagent ion and analyte ion clouds leads to a decrease in the frequency of collisions between reagent anions and analyte cations. For this reason, hybrid ETUVPD experiments were undertaken to evaluate the overall dissociation efficiency when the ET step was undertaken in the LIT (8 msec ET reaction time) versus the HCD cell (15 msec reaction period), in each case with UVPD performed in the HCD cell. Similar distributions and types of product ions were observed for both hybrid variations as illustrated for ubiquitin (13+) in **Figure 1.3**. For ETUVPD in which both ET and UVPD were undertaken in the HCD cell, a longer activation period was required to attain the same level of S/N due to the lower effectiveness of ET in the HCD cell, as mentioned above. The initial ETUVPD feasibility experiment provided evidence that there is little to no additional secondary fragmentation resulting in convoluting internal ions, an outcome consistent with prior results obtained using EThcD for peptides.[4,5] While internal ion formation can be used for diagnostic purposes in top down experiments with extensive *a priori* knowledge of the protein of interest,[21] accommodating internal ions in a high throughput identification search strategy would cause a prohibitively large increase in fragment ion search space.

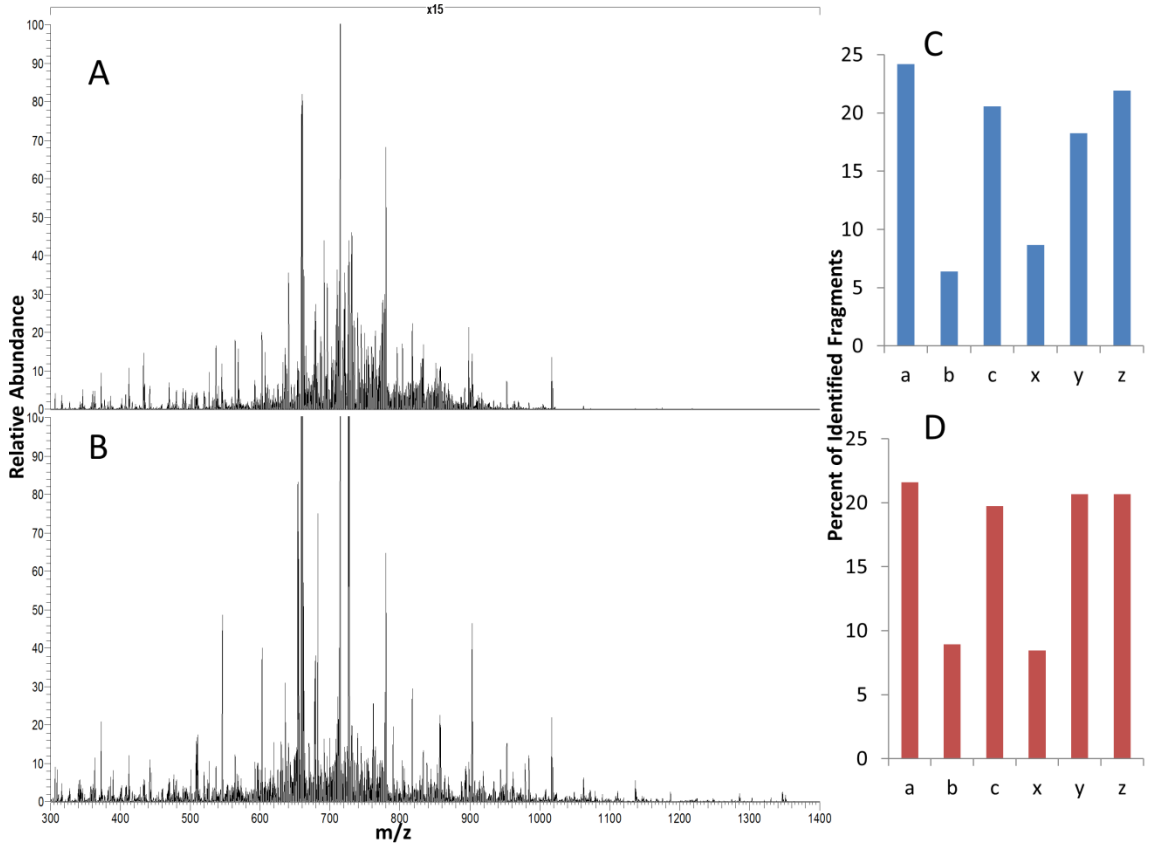

Figure 1.3. A) ETD performed in LIT (15 ms reaction time, reagent AGC 1E5) followed by isolation of m/z 659 ±300 in the LIT, then UVPD using one 2 mJ laser pulse in the HCD cell; B) ETD performed in HCD (15 ms reaction time) followed by one 2 mJ laser pulse in the HCD cell, for ubiquitin (13+). The corresponding fragment ion distributions are shown in C and D.

Performing MS/MS in the HCD cell allows trapping, activation and analysis of a wider m/z range of product ions compared to MS/MS undertaken in the LIT. Specifically, performing ETD in the LIT allows isolation and transfer to the HCD cell of a range of product ions $\pm$ 300 *m/z* units of the selected precursor ion, Undertaking ETD in the HCD cell and subsequent activation by UVPD does not require re-isolation after ETD, and so all product ions may be simultaneously trapped, activated and analyzed. This allows comparison of ETUVPD based on isolation of specific charge-reduced

precursors from ET or broad populations of ions encompassing nearly the entire product ion spectrum resulting from ETD. For example, ubiquitin was infused and the *z = 13* charge state was selected for ETD in the LIT, and the dominant product ions (as expected) were charge-reduced precursors (ETnoD). Subsequent photoirradiation of individually isolated singly, doubly, and triply charge-reduced species in the HCD cell resulted in mainly UVPD-type fragmentation, shown in **Figure 1.4A, 1.4B, and 1.4C**. The abundance of the intact charge-reduced proteins decreased with each electron adduction, and for that reason the signal-to-noise of the resulting fragment ions also decreased during the subsequent UVPD step, resulting in identification of only the most abundant fragment ions (**Figure 1.4F**). Also, since a large population of UVPD fragments have *m/z* values close to the precursor, fragment ions of higher *m/z* values are more likely to be identified upon photodissociation of more charge-reduced precursors (because the selected charge-reduced precursor and resulting fragment ion isotopes in lower charge states are less crowded and shifted higher in the *m/z* landscape) (**Figure 1.4C**).

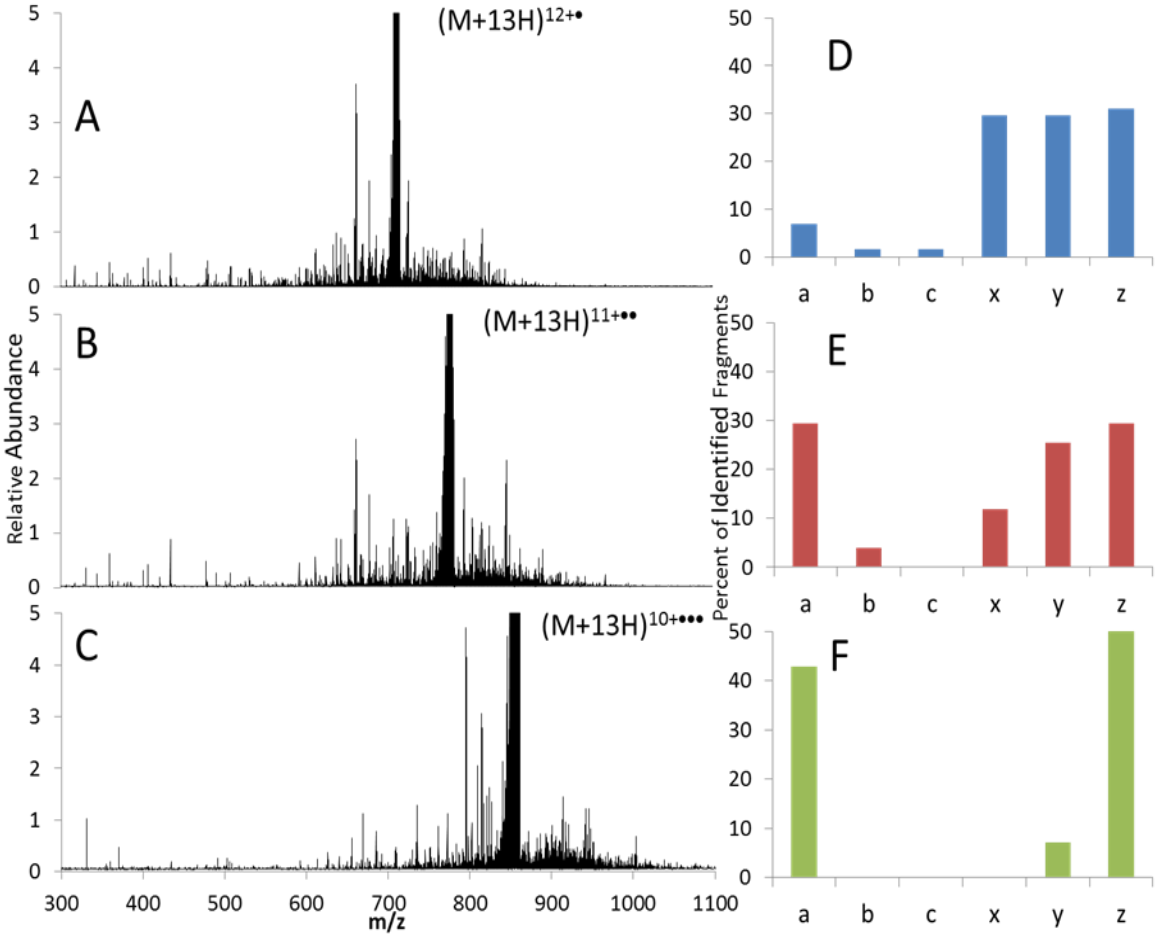

Figure 1.4. ETUVPD (8 ms ETD of ubiquitin (13+) in the LIT followed by one 1 mJ laser pulse in the HCD cell): A) 12+•, B) 11+••, C) 10+••• and corresponding distribution of ion types in D, E and F.

This latter benefit of ETUVPD is further illustrated in **Figure 1.5** for which the number of fragment ions specific to each activation method and their respective distributions across the *m/z* range from *m/z* 300 to 950 are shown. These results for individual charge-reduced precursors showcase the potential benefits of combining ETUVPD results from several charge states or ideally via analysis of multiple precursor charge states at once (as is possible in the HCD cell).

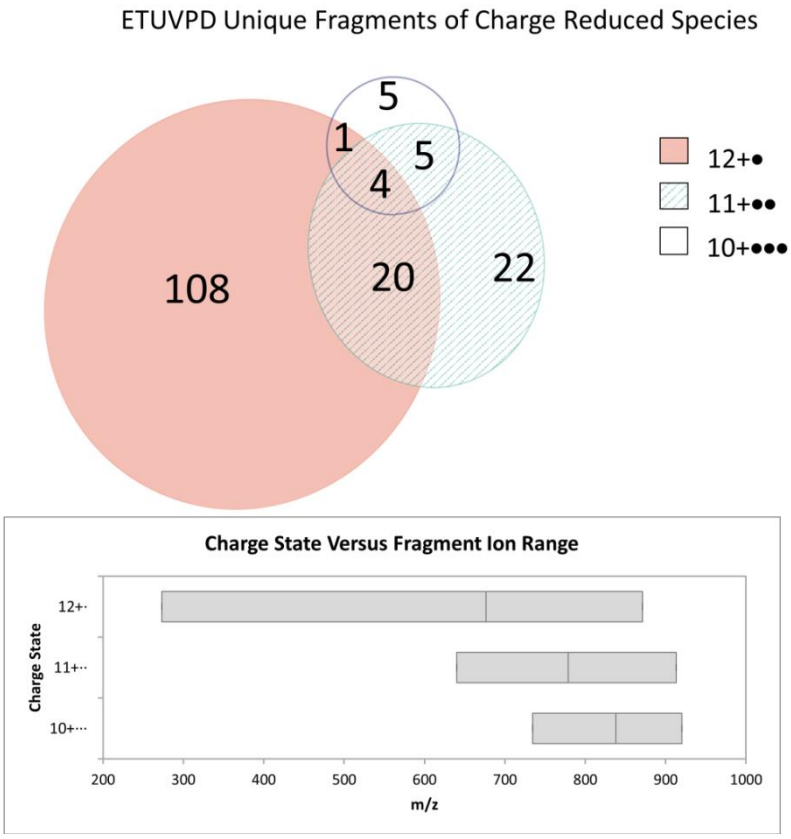

Figure 1.5. Top: Venn diagram depicting specific ion overlap between spectra resulting from UVPD of different charge-reduced species of ubiquitin including 12+., 11+.., and 10+… (top). Bottom: Graph demonstrating the corresponding m/z ranges of the identified fragment ions in each spectrum in which the bar spans the m/z range of the fragment ions and the vertical line represents the average fragment m/z value.

This strategy of simultaneous UVPD of a broader range of precursors and product ions was implemented and evaluated via ETD of the $z = 13$ charge state of ubiquitin in the HCD cell followed by UVPD of the entire population of both charge-reduced and non-reduced precursors as well as product ions arising from ETD. This "broadband" ion activation by UVPD offers two potential benefits. First, the total ion population available for UVPD activation is increased relative to UVPD of a single charge-reduced species.

Second, the potential for broad ion isolation in the HCD cell allows detection of a wider *m/z* range of product ions generated in the initial ETD reaction as well as the additional ones from UVPD. In the context of characterization of intact proteins, obtaining high sequence coverages and maximizing dissociation efficiencies are premium benefits, both of which are feasible with the broadband ETUVPD approach. To capitalize on these benefits, ETUVPD with broad ion isolation was undertaken for ubiquitin along with comparison to UVPD alone and ETUVPD with selected ion isolation (see **Figure 1.6**). Electron transfer activation in the HCD cell followed by a single 5 ns UV pulse (2.5 mJ) resulted in a fragment ion distribution that resulted from contributions from both ETD and UVPD (**Figure 1.6C**). **Figure 1.6** shows expansions of the spectral region from *m/z* 720 to 780 for UVPD (12+), ETUVPD in which the charge-reduced 12+• ions generated by ETD in the LIT were isolated and subjected to UVPD in the HCD cell, and for ETUVPD in which all the products arising from ETD of the 13+ ions of ubiquitin in the HCD were subsequently subjected to UVPD. The shaded regions are unique fragments not seen upon standalone UVPD or UVPD after isolation of the charge-reduced 12+• ions in the selective ETD/UVPD spectrum and are only observed upon broadband ETUVPD. Although many of the fragment ions are the same in all three spectra, the new ones generated upon ETUVPD using broad precursor isolation provide additional sequence coverage.

After demonstration of feasibility of ETUVPD and evaluation of initial metrics, all subsequent hybrid MS/MS experiments were performed via both ETD and UVPD in the HCD cell. Since UVPD occurs in the HCD cell, performing ETD in the same location alleviates the necessity of more time-consuming MS3 experiments (ETD in the LIT cell followed by transfer of ions and UVPD in the HCD cell) in data dependent LCMS runs. For experiments entailing ETD in the LIT cell and UVPD in the HCD cell,

the total time per scan is estimated as 1.636 sec, including an MS1 event to survey the available precursor ions, then an MS/MS event for ETD in the LIT with a 48 msec analytical scan to determine the ions created by ETD, then a third scan to repeat the ETD sequence, a short isolation period (4 ms) and transfer to the HCD cell (1-2 ms), then the UVPD period and mass detection. For ETUVPD in the HCD cell, the first scan is the same (MS1 scan to assess ion population), then there is an isolation/transfer sequence to transfer ions to the HCD cell, then the ETD/UVPD period and mass analysis for a grand total of 1.567sec. Implementation of the entire hybrid method in the HCD cell is thus better suited for chromatographic experiments that have duty cycle constraints, as shown later.

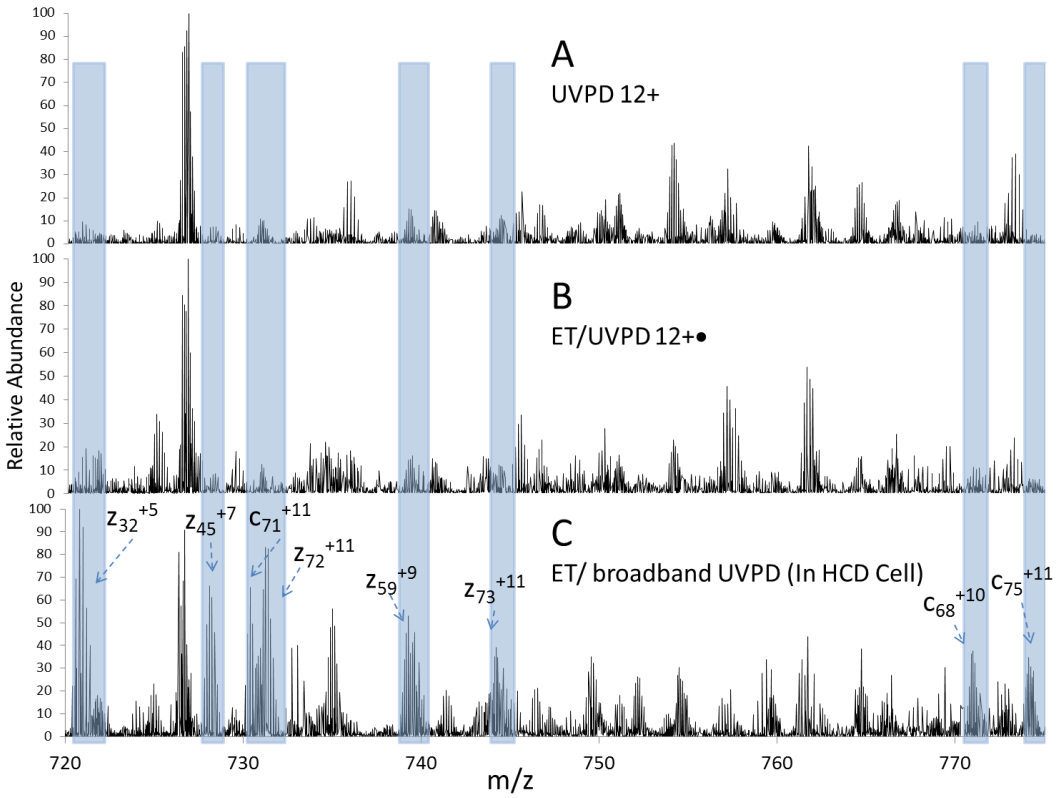

Figure 1.6. A) UVPD (one 2.5 mJ laser pulse) of ubiquitin 12+, B) ETUVPD (8 ms ETD in LIT of ubiquitin 13+ followed by one 1.8 mJ laser pulse of ubiquitin 12+•) (MS3), C) ETUVPD (15 ms ETD of 13+ ubiquitin in HCD cell followed by one 2.5 mJ laser pulse of all product ions).

ETUVPD Decreases Spectral Congestion

Although UVPD of intact proteins provides the richest spectra of any MS/MS method due to fragmentation at nearly every inter-residue position, a resulting complication is the spectral congestion and overlapping isotopic envelope of the fragment ions, thus requiring high resolution of the mass analyzer. The resolving power of Fourier transform mass analyzers is proportional to acquisition time, and for the crowded spectra that are produced by UVPD, maximum resolution is required. Heck and co-workers have shown previously that the ETD reaction for intact proteins in the HCD multipole is a slow reaction that culminates largely in charge-reduced peaks of the unfragmented

(intact) precursor.[11] While this outcome is not particularly beneficial for generating informative fragment ions, the result is quite advantageous for the hybrid ETUVPD method. The extent of spectral crowding and the difficulty associated with accurate deconvolution of the complex product ion spectra that result after UVPD have been reported previously using a set of green fluorescent protein (GFP) variants.[9] The assignable product ions were routinely biased toward lower charge states, even for interrogation of higher charge state precursors, due to the difficulty associated with effectively deconvoluting the higher charge products in the crowded spectra.[9] Taken together with visual inspection of the spectra and the total number of deconvoluted product ions (including those that were not matched to assignable fragment ions in the protein sequence), it is likely that the observed difficulty in deconvolution was the result of the combination of higher charge states (which have more closely spaced isotopic peaks) and product ions that overlap the same *m/z* region of the highly charged precursor.[9] For the present study, intact proteins of varying sizes were infused and analyzed in an optimized method in which both activation events were performed in the HCD cell prior to detection in the Orbitrap analyzer (**Figure 1.7**). Ubiquitin (8.5 kDa), myoglobin (16.9 kDa), and carbonic anhydrase (29 kDa) were activated using all methods under investigation; UVPD, ETD, and ETUVPD. In all cases, the greatest total number of matched fragment ions resulted from ETUVPD (as exemplified by the results for myoglobin in **Figure 1.7**). Visual inspection of the spectra in **Figure 1.7** clearly depicts how the ion current is distributed more effectively across the *m/z* landscape by combining the two activation methods. ETUVPD spectra from the $z = 22$ charge state of myoglobin showed not only a moderate increase in the number (and percentage) of matched fragment ions compared to UVPD or ETD alone, but also an increase in the total

number of deconvoluted ions and percentage of the fragment ions matched to the protein sequence.

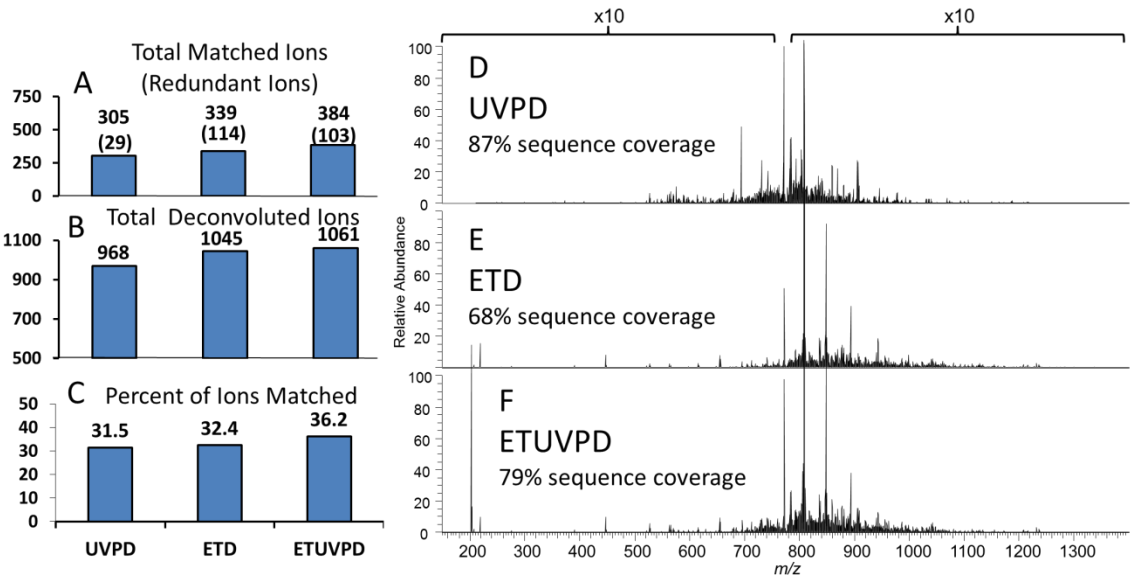

Figure 1.7. Shown for each of the three fragmentation strategies are (A) the total number of matched fragment ions (with the number of redundant ones shown in parentheses), (B) the total number of deconvoluted fragment ions (matched plus unmatched), and (C) the percent of fragment ions matched to the protein sequence (calculated by dividing the number of matched fragment ions by the total number of deconvoluted fragments). All results correspond to the z = 22 charge state of myoglobin (16.9 kDa). On the right are product ion spectra resulting from (D) UVPD, (E) ETD, and (F) ETUVPD of myoglobin (22+). All activation events were performed in the HCD cell.

The increase in the number of deconvoluted fragment ions was observed for both ETD and ETUVPD, an expected outcome owing to the ability of ETD to more effectively spread the ion current out across the *m/z* landscape via charge reduction. If this increase in the number of deconvoluted ions was accompanied by a substantial decrease in the percentage of those ions that were matched to the protein sequence, one could assume that the new ions were largely due to secondary or non-specific fragmentation, but

combining ETD with UVPD resulted in increases in the total number of deconvoluted fragments and in the percentage which could be matched to the protein sequence relative to UVPD alone. The increase in the number of deconvoluted fragment ions relative to UVPD alone corresponds to a more even distribution of 'true positive' fragment ions, further confirmed by evaluation of the standard deviation of both the abundances and the *m/z* distribution of all identified ions. UVPD still gave the best overall sequence coverage (87%) relative to ETD (68%) or ETUVPD (79%) for myoglobin.

With respect to the product ion abundances for each of the MS/MS methods, the average abundance was 4.0×10^3 ($\pm 7.7 \times 10^3$) for UVPD, 1.0×10^4 ($\pm 1.0 \times 10^4$) for ETD, and 7.7×10^3 ($\pm 9.4 \times 10^3$) for ETUVPD. The distributions of all matched product ions were grouped in 100 Th bins for each method (**Figure 1.8**).

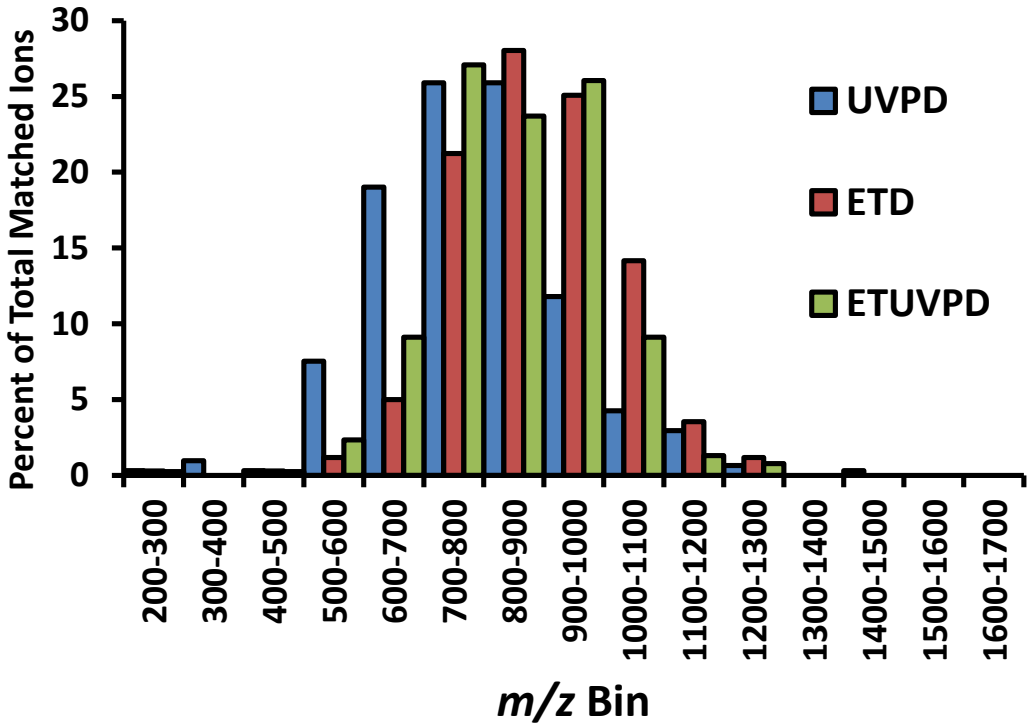

Figure 1.8. The product ion distribution across the m/z landscape upon dissociation of the z = 22 charge state of myoglobin using UVPD (blue), ETD (red), and ETUVPD (green).

The matched product ions fall into a greater number of bins for ETD and ETUVPD, thus indicating a broader distribution of product channels and more product charge states. These metrics reflect the ability of ETUVPD to enhance protein characterization by apportioning product ion current more evenly for both the *x* (mass to charge ratio) and *y* (intensity) variables, resulting in more informative spectra.

In this context, evaluation of the ion type distributions of the three model proteins reveals a trend towards more evenly distributed fragment ion pairs (i.e. *a/x, b/y, c/z*) for ETUVPD. Shown in **Figure 1.9** are the ion type distributions obtained using UVPD, ETD, and ETUVPD for each protein, which are abbreviated as U, M, and CA for

ubiquitin (averaging 13+, 12+, and 11+ precursor charge states), myoglobin (averaging 23+, 22+, and 21+ charge states), and carbonic anhydrase (34+), respectively.

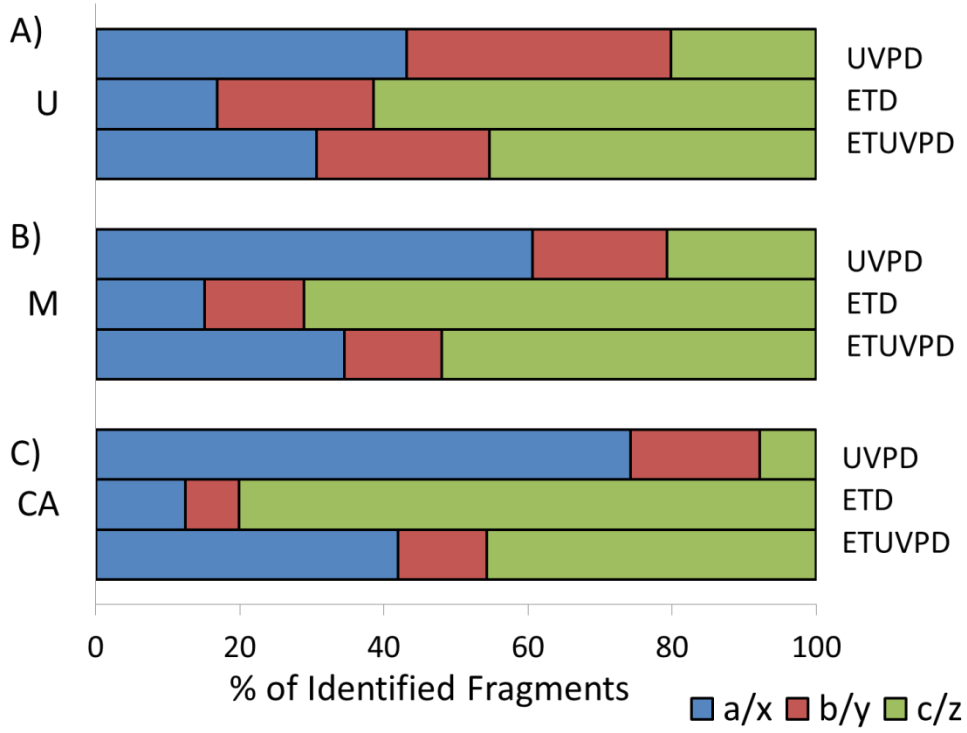

Figure 1.9. Shown are percentages of ion type pairs of total fragment ions identified by UVPD, ETD and ETUVPD for A) ubiquitin (U), B) myoglobin (M), and C) carbonic anhydrase (CA), with all activation events performed in the HCD cell (UVPD: one 2.5 mJ laser pulse; ETD: 15 ms; ETUVPD: 4 ms ETD and one 1.0 mJ laser pulse).

The distribution of fragments for UVPD is generally biased towards *a*- and *x*-type ions, especially as the protein mass increases. ETD resulted in a majority of *c*- and *z*-type ions, as expected. ETUVPD showed the most uniform distribution between *a*/*x* and *c*/z types, thus supporting the concept that ion types from both standalone UVPD and ETD are combined for the hybrid methods. Interestingly, the portion of N-terminal versus C-

terminal product ions does not vary significantly from UVPD to ETD to ETUVPD (**Figure 1.10**).

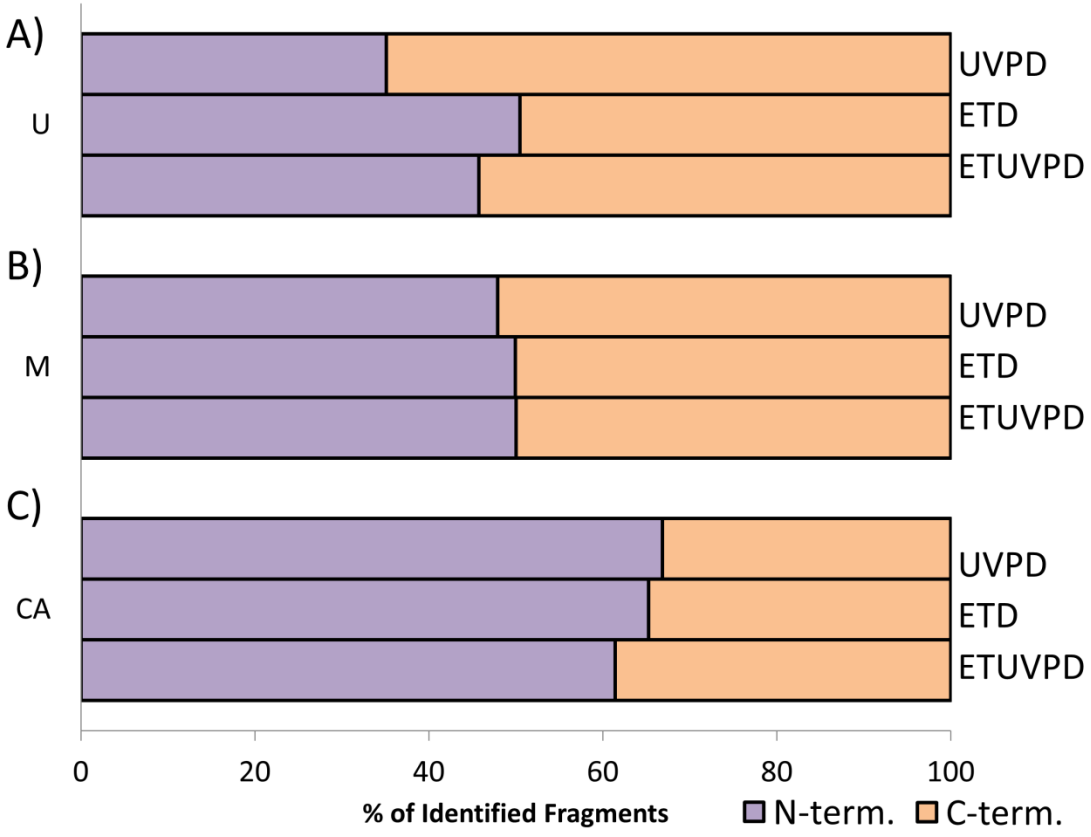

Figure 1.10. Shown are percentages of N- and C-terminal product ions upon UVPD, ETD and ETUVPD for A) ubiquitin (U), B) myoglobin (M), and C) carbonic anhydrase (CA).

In terms of sequence coverage (calculated based on the number of interresidue cleavages relative to the total number of interresidue backbone bonds), the coverages obtained for myoglobin (22+) were 87% for UVPD, 68% for ETD, and 79% for ETUVPD. For carbonic anhydrase (34+), the sequence coverages were 68% for UVPD, 62% for ETD, and 73% for ETUVPD.

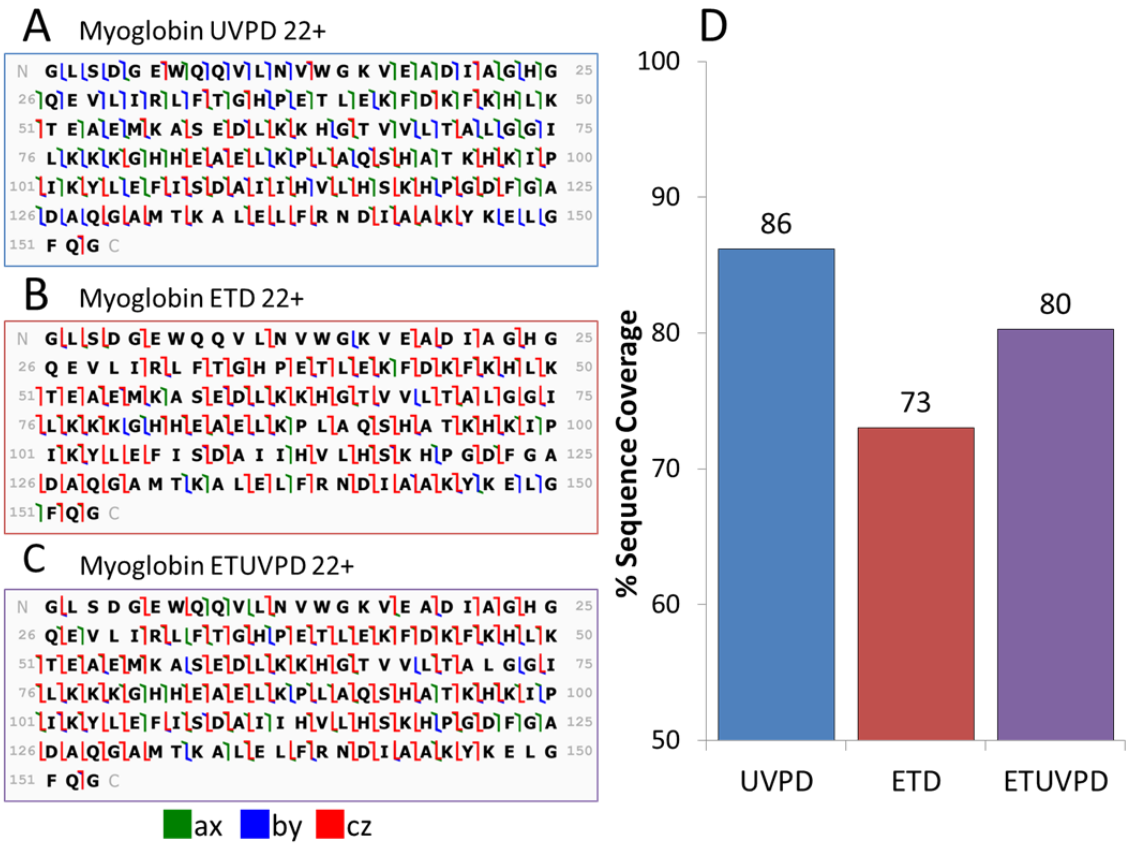

Figure 1.11. Shown for each of the three fragmentation strategies are sequence coverage maps for myoglobin (22+) for (A) UVPD, (B) ETD, (C) ETUVPD, and (D) sequence coverage percent comparison for all three activation types. All activation events were performed in the HCD cell.

The sequence maps for myoglobin and carbonic anhydrase are shown in **Figures 1.11** and **1.12**, respectively.

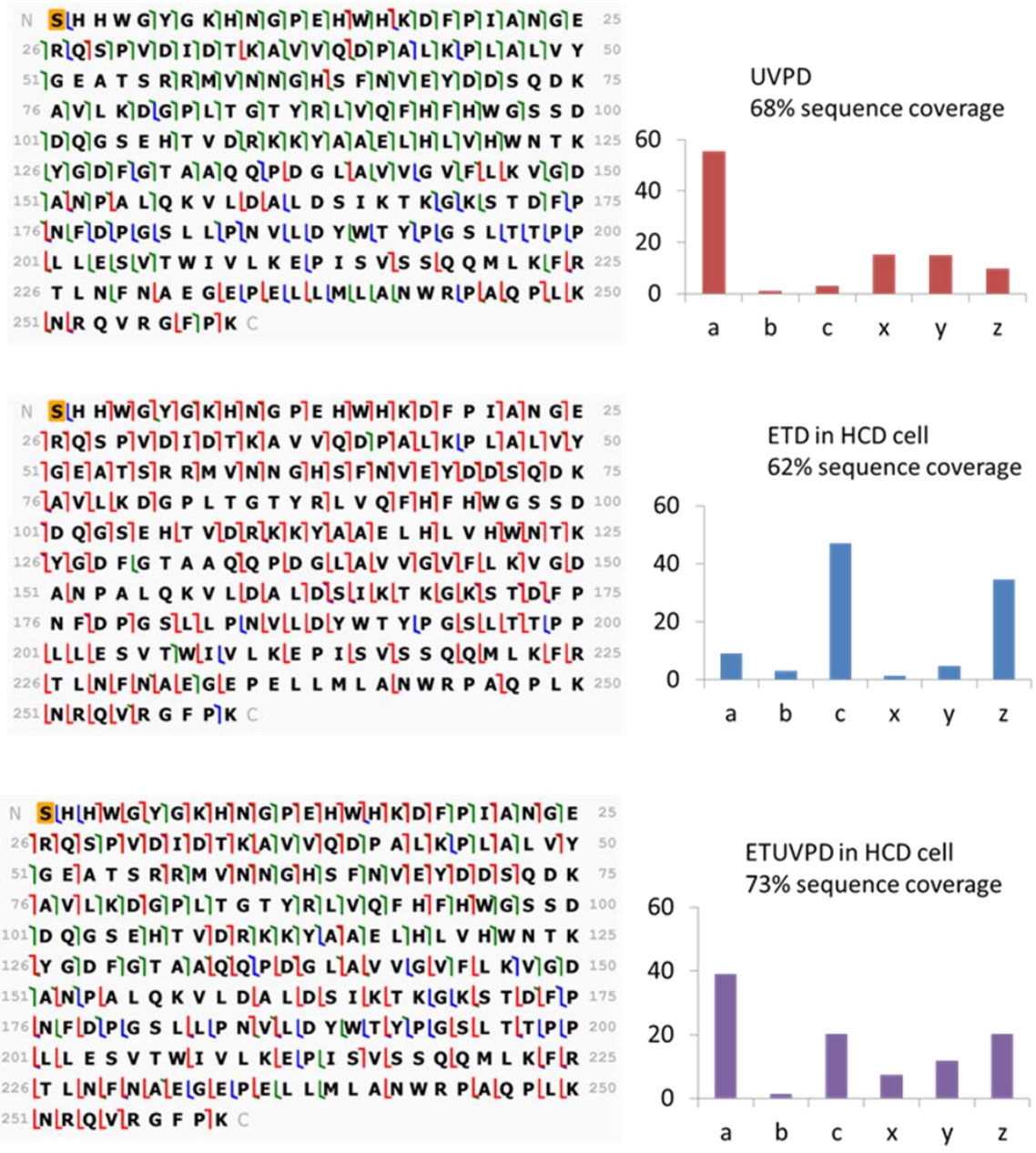

Figure 1.12. Shown for each of the three fragmentation strategies are sequence coverage maps for carbonic anhydrase (34+) for UVPD, ETD, ETUVPD, and corresponding distributions of ion types. All activation events were performed in the HCD cell.

Thus, although the distribution of ions changes for the hybrid method relative to UVPD or ETD alone, the net sequence coverage does not improve significantly.

LC-UVIETD and LC-ETUVPD

From the optimization and survey results for ubiquitin, myoglobin, and carbonic anhydrase, several sets of hybrid fragmentation conditions were chosen for analysis of the E. coli ribosome. The ribosomal proteome is composed of approximately 55 small and basic proteins. The positively charged Lys and Arg side chains interact with the rRNA phosphate backbone to maintain the ribosomal structure as a whole. This proteome is an ideal sample for evaluating the hybrid methods due to the likelihood of observing high charge states and the well-known positive correlation between precursor charge and ET reaction efficiency.[13] For this phase of hybrid activation experiments, all fragment ions (and non-dissociated and charge-reduced precursors) were simultaneously subjected to ETUVPD in the HCD cell. Additionally, further assessment of the impact of the ET reaction period on ETUVPD was undertaken for higher throughput LCMS applications. Using a digital delay generator, laser irradiation could be triggered either at the end of the electron transfer reaction period (termed ETUVPD, as described above) or at the beginning of the electron transfer reaction period (termed ultraviolet irradiation ETD or UVIETD), and the duration of the electron transfer reaction period could be varied. Two electron transfer reaction periods were chosen: 10 ms and 30 ms. A 10 ms period was chosen to maximize the production of intact charge-reduced proteins, and as such, distribute the ion current more effectively across the m/z landscape prior to UVPD. A 30 ms period was used to enhance the degree of radical-directed dissociation of the proteins in a manner complementary to the distinctive fragmentation promoted by UVPD.

Experiments utilizing all configurations (10 ms or 30 ms electron transfer period and preceded or followed by UVPD) were compared based on several metrics. The false discovery rate (FDR), average –log (E value) (where lower E values or higher –log (E values) reflect better matches), average number of fragments, and individual protein E values were compared to deduce which method was most ideally suited for combining both identification- and characterization-centric approaches. Interestingly, the FDR curves associated with all four iterations of the hybrid methods (ETUVPD 10 ms, ETUVPD 30 ms, UVIETD 10ms, and UVIETD 30 ms) resulted in nearly identical curves (see **Figure 1.13**).

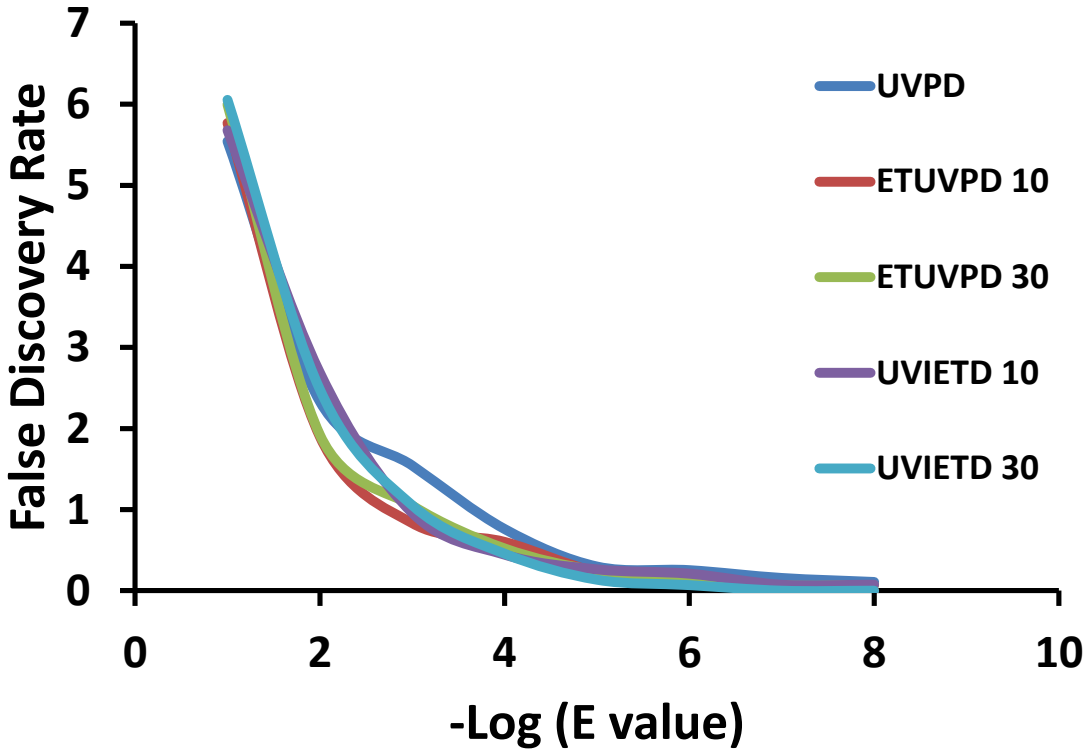

Figure 1.13. Shown are curves depicting the empirically derived false discovery rates associated with each method used on the E. coli ribosomal proteome.

The nearly identical FDR curves as well as the earlier infusion studies that confirmed similar percentages of matched ions (32% for UVPD compared to 36% for ETUVPD, **Figure 1.7**) indicate that there is a low degree of additional internal fragmentation resulting from ETUVPD. Internal fragments cause a massive increase in product ion search space that is prohibitive for high throughput analysis, and one could expect that sequential activation using two methods is more likely to result in this undesirable outcome. Our results show that ETUVPD does not result in extensive internal fragmentation. We have previously shown that the laser energy required for efficient photodissociation is roughly inversely proportional to protein mass, meaning that fragmentation of larger proteins (or polypeptides) is achieved with less energy deposition than that required for efficient fragmentation of smaller proteins (or peptides).[8] The lack of internal fragments observed from the hybrid formats can be explained by the propensity of each method alone to preferentially fragment larger (and more highly charged) polypeptides.

Among the proteins that were identified by all dissociation methods (n = 33 proteins, see **Table 1.1**), UVPD resulted in the highest average –log (E value) at 60, followed closely by the ETUVPD for 30 ms (58) and then UVIETD for 10 ms (58) (where a higher –log (E value) indicates a better match).

Description	UVPD	ETUVPD 10	ETUVPD 30	UVIETD 10	UVIETD 30
RL10	19	6	14	5	15
RL11	16	12	10	29	7
RL13	33	25	26	34	20
RL15	83	90	76	80	59
RL16	7	15	10	9	12
RL18	56	51	47	44	33
RL19	55	61	36	53	32
RL22	83	82	76	68	66
RL23	63	28	30	40	18
RL24	102	76	100	110	77
RL25	61	42	34	80	45
RL27	53	26	34	19	19
RL28	62	46	44	36	44
RL29	160	140	130	108	55
RL30	120	130	140	143	96
RL31	96	100	94	82	61
RL32	96	110	130	120	130
RL33	98	100	150	120	140
RL34	130	130	140	130	110
RL361	79	85	62	79	78
RL6	8	137	12	5	3
RL7	60	42	22	47	13
RS12	5	4	13	5	16
RS12	9	5	8	10	16
RS13	27	19	9	12	10
RS14	28	25	31	43	24
RS15	96	54	52	47	32
RS16	99	91	71	109	72
RS19	120	100	87	72	65
RS20	68	76	94	110	54
RS21	56	80	64	65	67
RS8	23	19	41	24	21
SRA	145	110	130	160	130

Table 1.1. Shown are the –Log (E value) of all E. coli ribosomal proteins identified by all methods interrogated.

As for the protein complement identified in all analyses, UVPD by itself achieved the best fragmentation outcomes (as defined by the best E values) for 11 of the proteins, UVIETD for 10 ms was optimal for 9 of them, and ETUVPD for 30 ms was the best option for 7 of them. Both ETUVPD for 10 ms and UVIETD for 30 ms were only best for 3 of the 33 proteins each. This disparity in which method is optimal can be attributed to the vastly different ion type distributions achieved with each method. Shown in **Figure 1.14** is the distribution of ion types for each method for the 33 protein identifications.

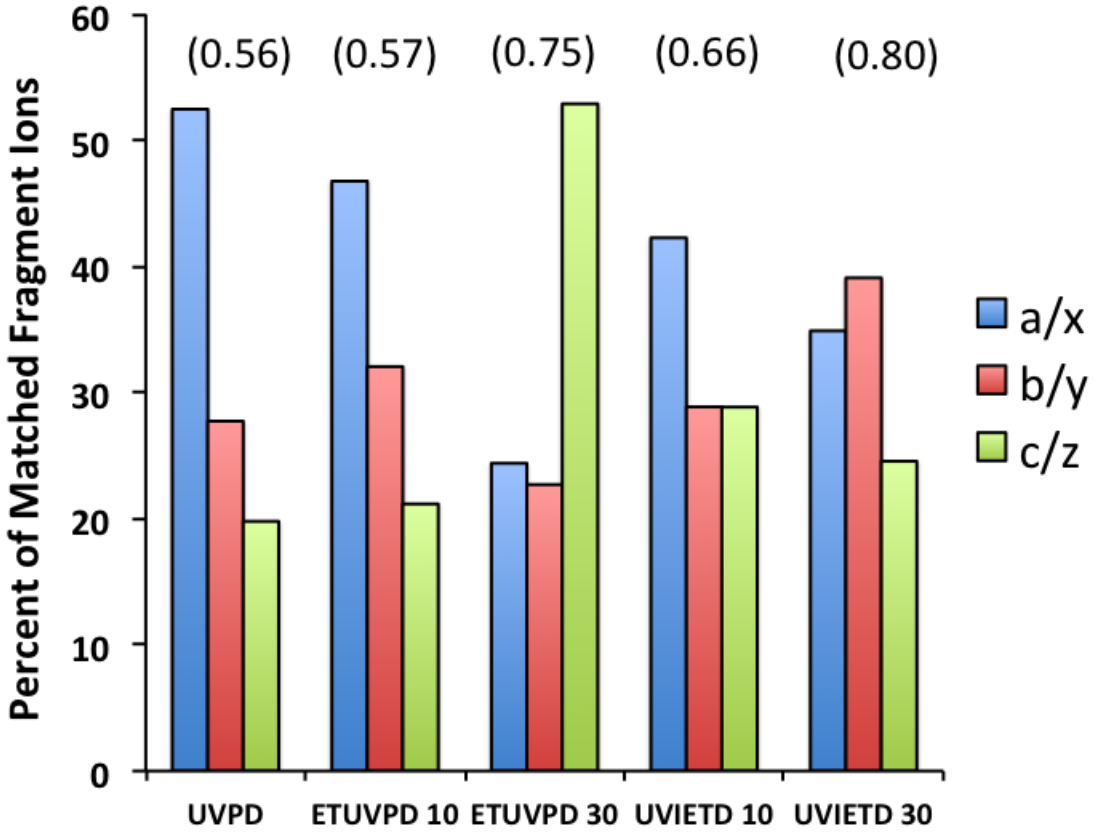

Figure 1.14. Histogram showing the distribution of ion types using UVPD and the hybrid methods for a ribosomal protein mixture. Shown above each set of bars in parentheses is the E value contribution per fragment ion.

From the fragment ion distributions shown in **Figure 1.14**, it is clear that hybridizing ETD with UVPD allows optimization of the ion population to suit the application. While one could argue that the total number of matched ions should be the only metric used to determine which method is best, changing the ion type distribution for higher confidence could be very useful for exploiting unweighted search algorithms. This is best exemplified by examining the average contribution of each matched fragment ion to the total E value for each identified protein ((-Log (E value)/number of identified fragments). For the UVPD data in **Figure 1.14**, the *a* and *x* type ions are dominant – typical of 'canonical' 193 nm UVPD. UVPD on average produced more than 95 fragment ions per protein identification; however, a large proportion of the ion current resided in *a* and *x* type ions which are sometimes duplicative for the same inter-residue position in the protein sequence. Comparing this to the results obtained by using UVIETD (10 ms), the average number of identified ions was lower (around 79), but it still gave the best score for 9 of the 33 proteins identified. The increase in the contribution of *c* and *z* type ions (which are not duplicative for the same inter-residue position) compensates for the overall lower total number of fragment ions and results in a positive impact on the E value per fragment ion. This simple calculation for these two methods revealed that the contribution per fragment to the E value using UVPD was 0.56 compared to 0.66 for UVIETD for 10 ms. In essence, this increase in the E value contribution per fragment underscores the possibility of achieving greater sensitivity via creating fewer fragment ions but ones with a more optimal distribution of ion types. UVPD alone of the *E. coli* ribosome provides a high level of protein identification and characterization but is dominated by *a* and *x* type ions,[10] as re-confirmed in this study. The primary utility of using hybrid ET_UVPD activation is the ability to modulate the fragmentation distribution more evenly among identifiable ion types.

CONCLUSIONS 1.5

Presented is a new method that combines ETD and UVPD simultaneously performed in the HCD cell of an Orbitrap Elite mass spectrometer to provide a more balanced contribution from each complementary pair of ion types, and specifically, to increase the contribution of *c*- and *z*-type ions. Pilot studies on several benchmark proteins of varying size as well a mixture of intact ribosomal proteins demonstrated the utility of ETUVPD and UVIETD as compelling methods for enhancing top down protein characterization. The enhancement arises from the production of a more diverse set of ion types facilitating characterization via representation of overlapping sections of the protein sequence from both termini, especially when exploiting the advantage of the ultrahigh resolution available in single protein infusion experiments. Additionally, the ETUVPD and UVIETD approaches demonstrate successful hybridization of activation methods with the ability to modulate the activation time in the ETD step to achieve the preferred ion types characteristic of either ETD or UVPD.

Chapter Two: Ultraviolet Photodissociation of Protonated, Fixed Charge, and Charge-Reduced Peptides

OUTLINE 2.1

The fragmentation behavior of three peptides (RGAFSTFGAS, GAFSTFGASR, and GAFSTFGASS) was evaluated by collisional activated dissociation (CAD), higher energy collisional activated dissociation (HCD), and ultraviolet photodissociation (UVPD) and hybrid methods combining electron transfer with CAD, HCD, or UVPD in order to assess the impact of the location of a basic site at the C- or N-terminus, the presence of a fixed charge at the C- or N-terminus, and the presence of a radical site. The release of a mobilized proton occurred for those peptides modified with a quaternary amine at the C- or N-terminus, thus resulting in formation of C- and/or N-terminus fragment ions that would not otherwise be expected if the fixed charge remained static. Activation of charge-reduced peptides (i.e. peptide radical ions) resulted in simplified spectra compared to the corresponding even electron peptides. Interestingly, UVPD of the charge-reduced species generated similar spectra to CAD and HCD of the same precursor ions, suggesting a shift to dominant radical-induced dissociation rather than the more diverse pathways common upon photodissociation.

INTRODUCTION 2.2

Bottom-up proteomic strategies, those that rely on proteolytic digestion of proteins and tandem mass spectrometry to characterize the resulting peptides, are the most popular approaches for implementation of high throughput, broad-scale identification of proteins in complex mixtures.[22-24] The typical bottom-up workflow has proven successful for identifying hundreds to thousands of proteins in complex mixtures based on matching peptides to proteins via *in silico* database search algorithms. The foundation of the database search algorithms rests in large part on the ability to generate

accurate theoretical tandem mass spectra based on predictive rules of peptide fragmentation.[25-28] Understanding the factors that modulate peptide dissociation remains an important challenge in developing the best correlations between experimental MS/MS spectra and *in silico* predictions. Both the location and type of peptide charge sites, as well as the ion activation method, influence the resulting fragmentation patterns. As one example, the most common bottom-up protocol involves proteolytic digestion using trypsin which cleaves peptide bonds at the basic amino acids lysine and arginine.[29] The presence of basic amino acids can alter MS/MS fragmentation patterns by sequestering a proton,[26] thus reducing proton mobility and simplifying spectra by restricting the array of pathways within a particular energy range. Others have noted the enhancement of specific peptide backbone cleavage sites, such as cleavages adjacent to acidic residues and at the N-terminal side of proline, among others, that lead to especially prominent fragment ions in the MS/MS spectra of protonated peptides.[27-30]

Attaching fixed charges to peptides through derivatization has also been shown to modulate the formation of N- and C-terminal fragment ions via charge-remote mechanisms, as reported by a number of groups.[31-55] Fixed charges were originally added to peptides and other molecules primarily as a means to enhance their ionization efficiencies, typically for matrix assisted laser desorption ionization (MALDI) methods.[49,54] However, at the same time it was noted that the resulting fixed charge peptides exhibited differences in their fragmentation behavior compared to the analogous non-fixed charge counterparts. For example, the Reilly group has investigated several fixed charge reagents and found that the presumed fixed charge site of a quaternary amine modification can cleave, generating a mobile proton and leading to fragment ions that do not originate from the original fixed charge site.[45] Similar experiments with another fixed charged reagent, tris(2,4,6-trimethoxy phenyl)phosphonium acetyl (TMPP),

did not result in a similar mobile proton effect upon collision activated dissociation (CAD), except when arginine was located next to the fixed charge in the peptide sequence.[45] High energy ultraviolet photodissociation (UVPD) using 157 nm photons promoted consistent charge-remote fragmentation for TMPP-tagged peptides.[50] Additionally, UVPD activation of TMPP-tagged peptides exhibited side-chain losses, adding complexity to the MS/MS spectra.[50] Thus, evidence for variations in peptide fragmentation patterns has been correlated with the type of charge site (e.g. fixed charge versus mobile proton), the locations of charge sites (e.g. C-terminus, N-terminus, side-chain, backbone site), and the nature of the energization (e.g. low energy step-wise CAD versus high energy UVPD).

Affixing a fixed-charge tag to the N-terminus of a peptide has also been reported to improve sequence coverage obtained by electron transfer dissociation (ETD) for tryptic-like peptides (ones containing arginine at the C-terminus).[43] The fixed-charge tag was postulated to overcome some of the suppression of fragmentation that is commonly observed for histidine-containing peptides upon ETD. Additionally affixing charge tags to peptides resulting from tryptic digests of bovine serum albumin (BSA) resulting in greater sensitivity of multiple reaction monitoring analysis as well as identification of peptides not detected without the fixed charge tags.[55] When the charge tag was attached to the N-terminus of the peptide, dominant *a*-type ions were produced upon ETD due to the immobilization of charge at the N-terminus.[55]

Whether the peptides are odd electron radical ions or even electron species is an additional mitigating factor that has generated considerable interest in recent years with the emergence of electron-activated dissociation methods: electron capture dissociation (ECD)[1,56] and electron transfer dissociation (ETD),[2,58] Electron-activated methods lead to peptides with an extra electron via an exothermic electron transfer process that facilitates

radical-induced dissociation and production of *c-/z*-type fragment ions that contrast to the conventional *b-/y*-type fragment ions generated by collision-based methods. Although the electron-activated methods often favor the formation of non-dissociated charge-reduced precursor ions (i.e. ETnoD), fragmentation efficiency has been significantly enhanced by applying supplemental energy or by following electron-activation with an auxiliary activation method.[58] McLafferty and co-workers were the first to propose that supplemental heating or energization of ions during ECD could disrupt the noncovalent interactions that held non-dissociating ions together, thus increasing the formation of diagnostic fragment ions.[18] Because of the greater propensity of ions in low charge states to undergo charge reduction rather than fragmentation into *c/z* ions, a number of groups have developed means to increase the charge states of ions via using super-charging ESI conditions or by covalent attachment of fixed charge sites.[59-61]

In addition, "hybrid" activation methods that combine electron transfer reactions with CAD, higher-energy collisional dissociation (HCD), infrared multiphoton dissociation (IRMPD) or UVPD have been reported to circumvent some of the potential charge-dependent shortcomings of ECD or ETD alone and generate richer fragmentation patterns.[4,5,6,18,21,58,62-65] For example, we have previously used UVPD at 193 nm to explore the fragmentation of radical peptide cations generated by electron transfer reactions of protonated peptides.[7] A key feature that influenced the types of products was the position of the charge site as evidenced by the location of a sequestered proton (via a basic Arg residue) at either an N-terminal or a C-terminal arginine residue. When the proton was sequestered at the N-terminus for the peptide radicals, C_α-C(O) bond cleavages were favored, yielding *a*-type ions similar to those observed upon UVPD of protonated peptides.[7] When the proton was sequestered at the C-terminus, N-C_α cleavages were preferred, giving *z*- and *c*-type products more typically observed upon dissociation of

hydrogen-rich radical ions (as for ETD, ECD, or ETcaD).[7] A recent study utilized ETD and subsequent activation by CAD or UVPD to determine the impact of the location of a specific amino acid (serine) within a peptide sequence on the resulting peptide fragmentation patterns.[66] Interestingly, ETD yielded product ions that were responsive to 355 nm UV photoirradiation, whereas peptides did not normally absorb at that wavelength unless specifically modified with a chromophore. For peptides containing histidine, electron transfer reactions caused a chromophore effect that specifically enhanced absorption of 355 nm photons.[67]

We have recently reported an increase in sequence information obtained for intact proteins by combining ETD and 193 nm UVPD to produce more evenly distributed fragment ion types.[62] In general, 193 nm UVPD have been previously shown to yield dominant *a*-type fragment ions relative to other ions generated in top-down MS/MS analysis of proteins,[8,11] and thus the hybrid ETD/UVPD strategy provided a means to modulate the product ion distributions. In the present study we evaluate the variations in fragmentation of fixed-charge peptides in comparison to analogous peptides containing a highly basic, proton-sequestering arginine at the N- or C-terminus. The three reactions used to attach fixed charges are shown in **Scheme 2.1**. Three methods, CAD, HCD, and UVPD, are used to characterize the conventional protonated and fixed-charge peptides, and three hybrid activation methods, ETcaD, EThcD, and ETuvPD, are used to produce and analyze the corresponding peptide radical ions after charge reduction. To explore the impact of the location and type of charge on the fragmentation pathways of peptides, three peptides (RGAFSTFGAS, GAFSTFGASR, and GAFSTFGASS) were evaluated. Two of these peptide sequences were specifically designed to have a highly basic site (Arg) at the N- or C- terminus, and the third was an analogous peptide with no basic site. For all three peptides, the remainder of the peptide sequence was kept constant to

mitigate the impact of other residue-specific effects. UVPD has been shown previously to produce rich fragmentation patterns.[7,8,11,68-82] In the present study, it is shown that simplified spectra are produced by photodissociation of the charge-reduced fixed-charge peptides generated by ET reactions.

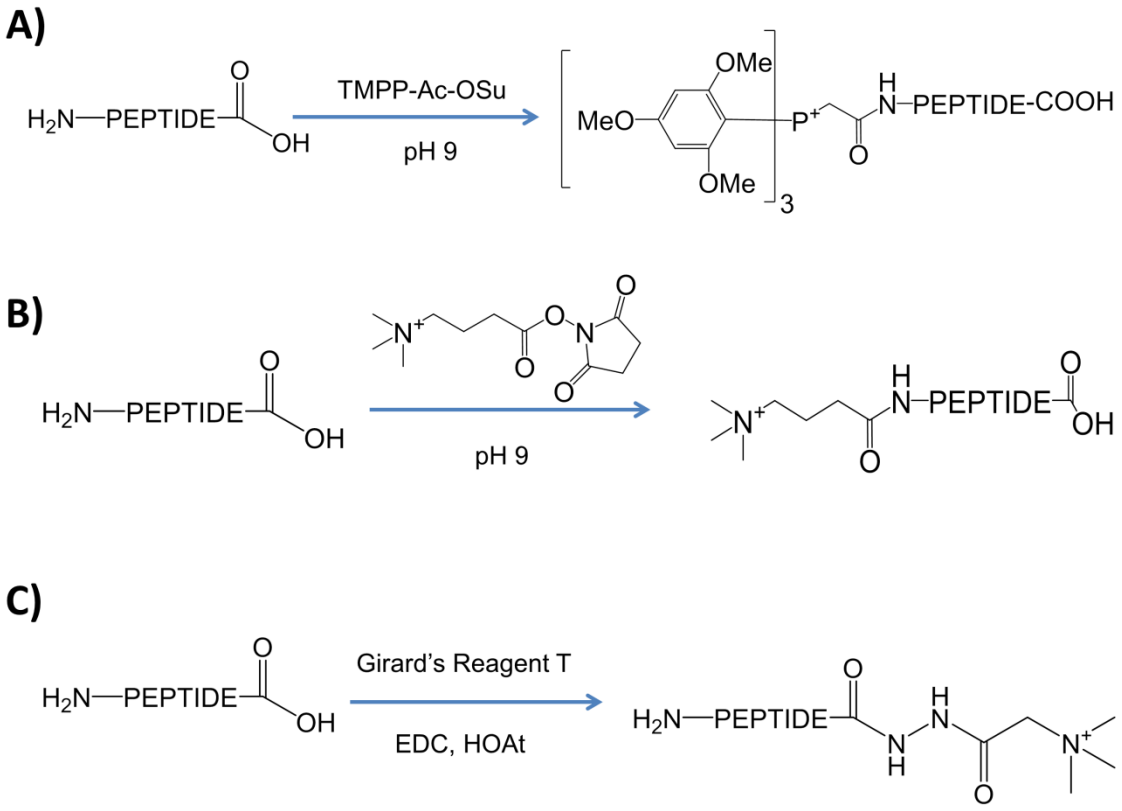

Scheme 2.1. A) Attachment of phosphonium fixed charge to the N-terminus of a peptide. B) attachment of a quaternary amine fixed charge to the N-terminus of a peptide, and C) attachment of a quaternary amine fixed charge to the C-terminus of a peptide

MATERIALS AND METHODS 2.3

Materials

N,N-Dimethylformamide (DMF), HPLC grade water, methanol and acetonitrile were obtained from Fisher Scientific (Pittsburgh, PA, USA). N-(3-Dimethylaminopropyl)-N′-ethylcarbodiimide hydrochloride (EDC) and 1-hydroxy-7-azabenzotriazole (HOAt) were purchased from AAPPTec, LLC (Louisville, KY, USA). N-Succinimidyl [tris(2,4,6-trimethoxyphenyl)phosphonio]acetate bromide (TMPP-AC-OSu) was obtained from Toronto Research Chemicals Inc. (Toronto, ON, CAN). Girard's Reagent T and trifluoroacetic acid were obtained from Sigma-Aldrich (St. Louis, MO, USA). Peptides RGAFSTFGAS, GAFSTFGASR, and GAFSTFGASS, were synthesized in-house using solid phase reaction and Fmoc amino acids from Novabiochem (Billerica, MA, USA).

Fixed Charge Derivatization of Peptides

Aliquots of each peptide were derivatized to contain a phosphonium N-terminal fixed charge via reaction with TMPP-AC-OSu using a previously described method (see **Scheme 2.1A**).[51] The molar stoichiometric ratio of the reaction was reduced to 5:1 (reagent:peptide) to decrease the residual TMPP that carried over after C_{18} cleanup. An additional peptide N-terminus fixed charge reagent, trimethyl-ammonium butyric acid with an amine-reactive N-hydroxysuccinimide group (TMAB-NHS), was synthesized in-house according to a previously reported method.[52] TMAB-NHS was reacted in a 5:1 stoichiometric ratio (reagent:peptide) in 0.2 M $NaHCO_3$ in 20% acetonitrile, pH = 9, using the reaction procedure also used to derivatize peptides with TMPP-AC-OSu (see **Scheme 2.1B**).[51] Quaternary amine fixed charges were attached to the C-termini of peptides by incubating a 100 μL aliquot of peptide (1 mM) in water with 100 μL of 10

mg/mL Girard's Reagent T (in 50% DMF). The reaction entailed mixing 100 μL of 15 mg/mL EDC in DMF, 100 μL of 15 mg/mL HOAt in DMF, and 30 μL of 10% TFA for a net pH of 6 (see **Scheme 2.1C**). The mixture was allowed to react for 12 hours at 35°C and dried under vacuum overnight. The resulting derivatized peptides were desalted using standard SPE C_{18} clean-up procedures.

Instrumentation and Data Collection

Derivatized and underivatized peptides were diluted to 1 μM with methanol/water/formic acid (70/30/0.1, v/v/v) before direct infusion into a Thermo Fisher Scientific Orbitrap Elite mass spectrometer (Bremen, Germany) modified to allow UVPD in the HCD cell as described previously.[8] A 500 Hz Coherent Excistar ArF (193 nm, 5 nsec per pulse) excimer laser (Santa Clara, CA, USA) was used for UVPD. The ion trap control language (ITCL) was customized to allow MS^3 combining ET reactions and UVPD. Hybrid MS^3 activation was undertaken by performing ETD of the +2 charge state precursor in the linear ion trap, followed by CAD (also in the linear ion trap), HCD (in the HCD cell), or UVPD (in the HCD cell) of the resulting isolated charge-reduced species. For comparisons of MS/MS behavior, CAD, HCD, and 193 nm UVPD spectra of each singly protonated or fixed charge peptide were collected. The CAD parameters were as follows: 23 - 35 NCE, activation time of 10 ms, and an activation q of 0.25. The HCD parameters were as follows: 23 – 38 NCE, activation time of 0.10 ms, and an activation q value of 0.25. 193 nm UVPD was undertaken by exposing the ions to 4 – 8 laser pulses at 2 - 3 mJ per pulse. The laser pulses were applied at 500 Hz during an 8 - 16 ms activation period.

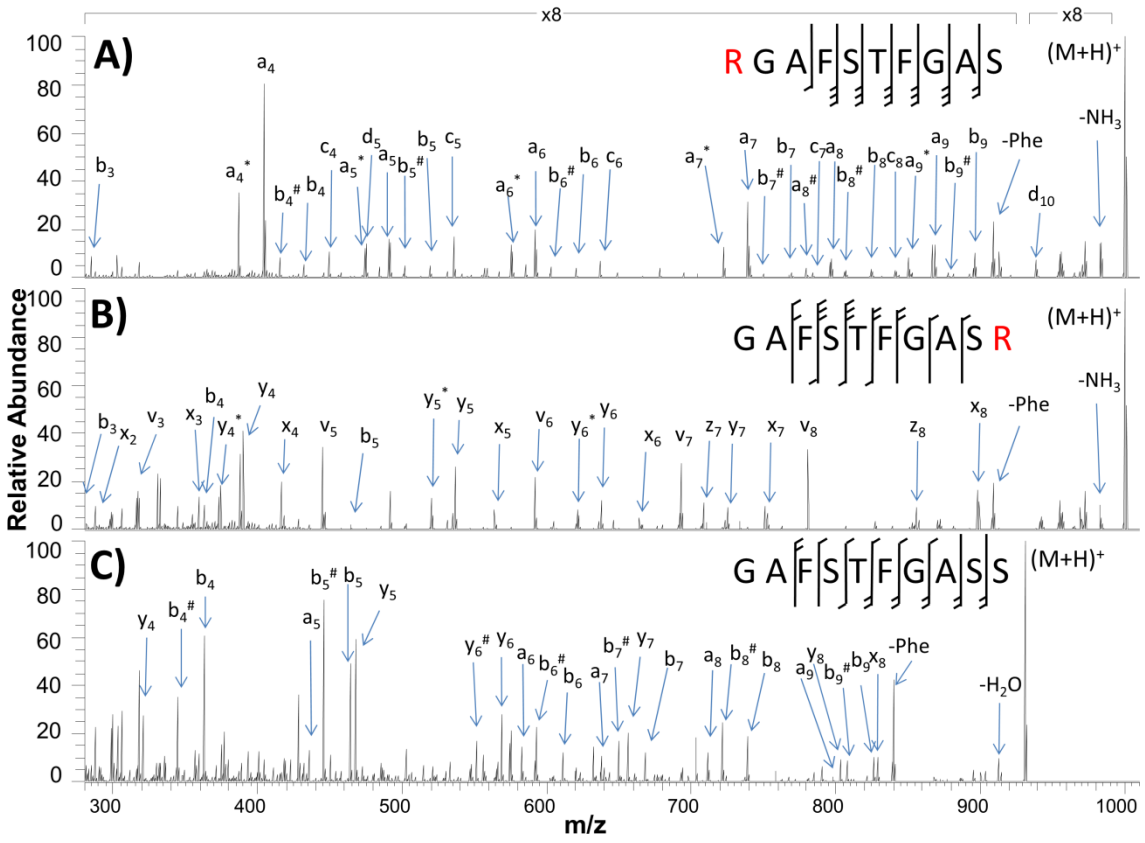

Figure 2.1. UVPD of protonated peptides: A) RGAFSTFGAS, showing mainly N-terminal fragments, B) GAFSTFGASR, showing mainly C-terminal fragments, and C) GAFSTFGASS, showing a mixture of both N and C-terminal fragments. All spectra have the same magnification scale (x8). # = water loss, * = ammonia loss.

RESULTS AND DISCUSSION 2.4

Comparison of the fragmentation patterns were assessed for three peptides (RGAFSTFGAS, GAFSTFGASR, and GAFSTFGASS) with or without a fixed charge attached at either termini and each one analyzed as either a singly protonated species (for those not modified with a fixed charge tag), a fixed charge ion (not protonated; the charge is appended via the phosphonium $TMPP^+$ or a quaternary amine QA^+), or a charge-reduced protonated radical ion (formed via an electron attachment reaction of a

protonated species). Singly protonated or fixed-charge peptides were produced by conventional ESI (with the fixed charges attached by derivatization reactions in solution as described in the experimental section). The peptide radical ions were generated in the dual-pressure linear ion trap of the Orbitrap Elite mass spectrometer through electron transfer (ET) reactions of the doubly charged peptides initially generated by ESI, resulting in charge-reduced peptide radical ions (i.e. initially 2+ but with an extra electron attached).[58] Subsequent activation of the resulting peptide ions was undertaken either in the high pressure trap (CAD) or in the HCD cell (for HCD or UVPD). Whether protonated, fixed charge, or charge-reduced, in each case the net charge state of the precursor ion was 1+, thus maintaining charge parity throughout the study.

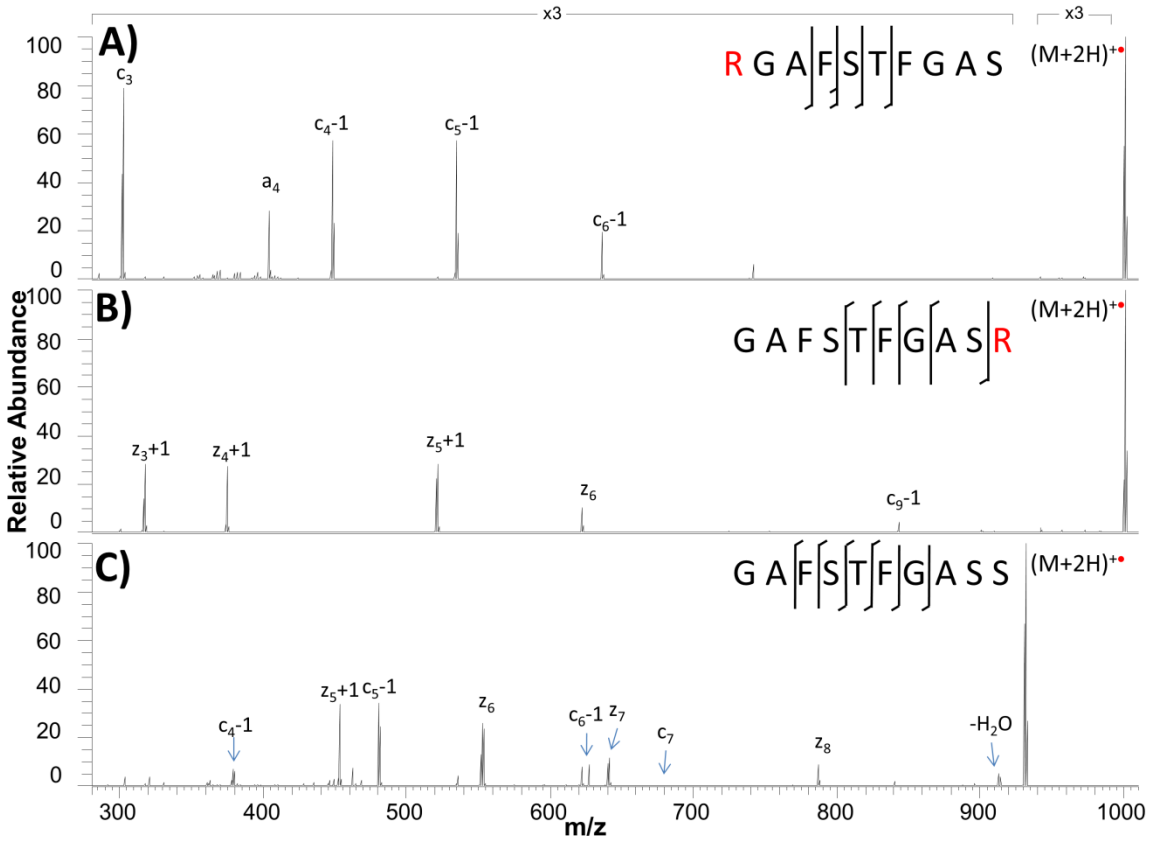

Figure 2.2. ETuvPD of protonated charge-reduced peptides: A) RGAFSTFGAS, showing mainly N-terminal fragments, B) GAFSTFGASR, showing mainly C-terminal fragments, and C) GAFSTFGASS, showing a mixture of both N and C-terminal fragments. All spectra have the same magnification scale (x3).

Representative examples of the MS/MS spectra are shown in **Figures 2.1 – 2.5** and **Figures 2.7 – 2.10**. **Table 2.1** provides a global summary of the types of fragmentation pathways observed for the peptides, in terms of formation of conventional sequence ions *(a,b,c, x, y, z)*, prominent neutral losses (-59 Da for those containing a quaternary trimethyl ammonium ion terminus), or formation of a significant TMPP ion (for the TMPP-modified peptides). Shown in **Figure 2.6** is a bar-graph summary of the number of N-terminal (*a,b,c*) and C-terminal (*x,y,z*) fragment ions for the three peptides

in their protonated, fixed charge, or odd electron charge-reduced forms. The presence of an N-terminal arginine or an N-terminal fixed charge led to the predominant formation of N-terminal fragments for all activation methods, whereas the presence of a C-terminal arginine or C-terminal fixed charge produced more C-terminal fragments. In each case, 193 nm UVPD produced a greater number of diagnostic fragments compared to CAD or HCD for the protonated or fixed-charge peptides. For the charge-reduced peptides, the number and types of fragment ions were very similar for all three activation methods: ETcaD, EThcD, and ETuvPD.

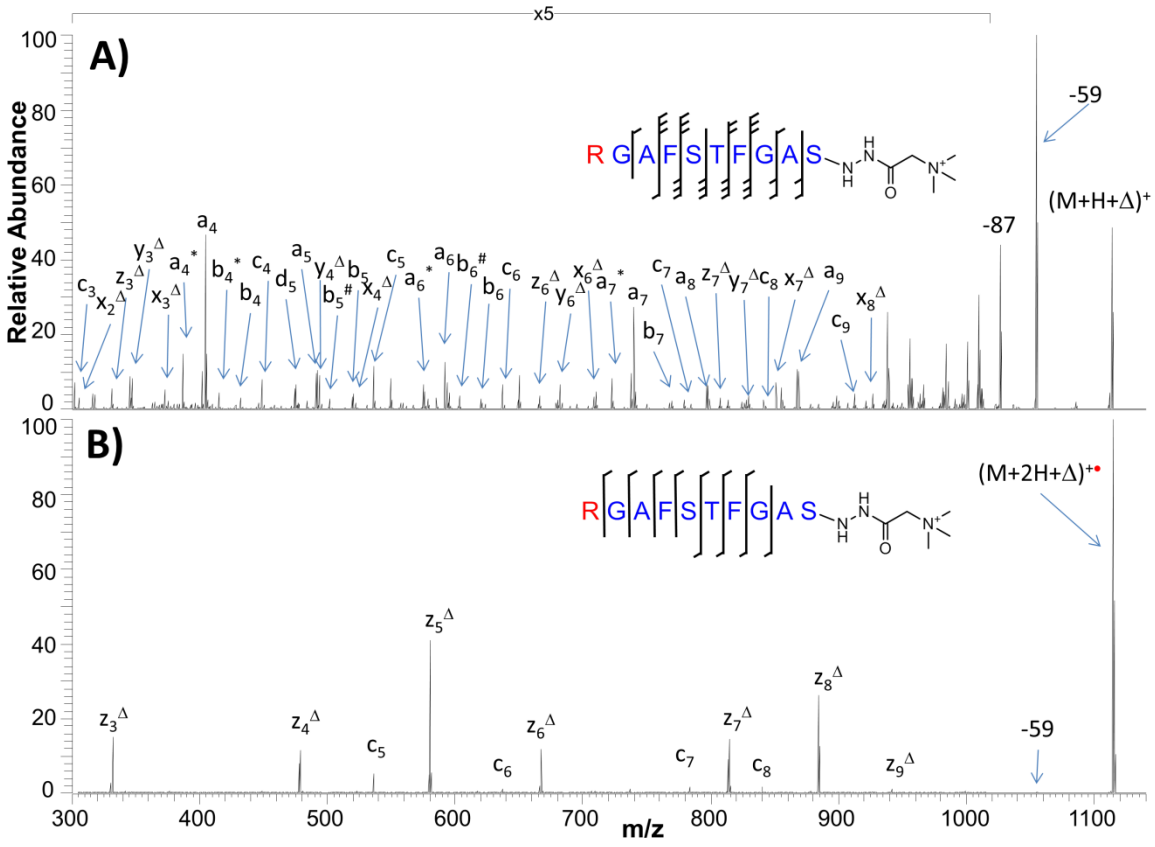

Figure 2.3. A) UVPD of +1 ion of C-terminal fixed-charge peptide RGAFSTFGAS-QA+ showing dominant loss of trimethyl amine, and B) ETuvPD of charge-reduced species of C-terminal fixed-charge peptide RGAFSTFGAS-QA+ simplified fragmentation. Δ = ions containing fixed-charge tag. All spectra have the same magnification scale (x5). # = water loss, * = ammonia loss.

As initial benchmark data, examples of the UVPD spectra obtained for singly protonated peptides containing a basic amino acid (arginine) at the N- or C-terminus are shown in **Figure 2.1** and the corresponding ETuvPD spectra (i.e. formation and analysis of the charge-reduced peptides) are shown in **Figure 2.2**. The UVPD mass spectra of protonated peptides are rich, containing *a,b,c, x, y,* and *z* ions, as well as side-chain loss ions (*d, v*). Neutral losses of water or ammonia from these primary fragment ions are also observed. These types of complicated fragmentation patterns are one of the

hallmarks of UVPD and are attributed to the multiple mechanisms of UVPD, occurring both directly from excited states and after intramolecular vibrational redistribution after internal conversion.[9,85] As expected, the presence of the terminal arginine shifts the distribution of N- and C-terminal fragments due to proton sequestration.[26] The presence of an N-terminal arginine results in production of solely N-terminal fragments (*a,b,c,d*) (**Figure 2.1A**), whereas a C-terminal arginine results in predominantly C-terminal fragments (*v,x,y,z*) and a few *b* ions (**Figure 2.1B**). For the peptide lacking an arginine, a more even distribution of N-terminal and C-terminal ions was observed (**Figure 2.1C**). The presence of side-chain fragments (*e.g. d* and *v* ions) during UVPD results from secondary charge-remote fragmentation of radical ions generated by the high energy deposition (6.4 eV) characteristic of 193 nm photons.[7] Biemann *et al*. have previously reported mechanisms for *d*- and *v*-type ions caused by high-energy CAD (10 keV) side-chain cleavages of *a*-type, and *y*- and *x*-type fragment ions respectively.[83]

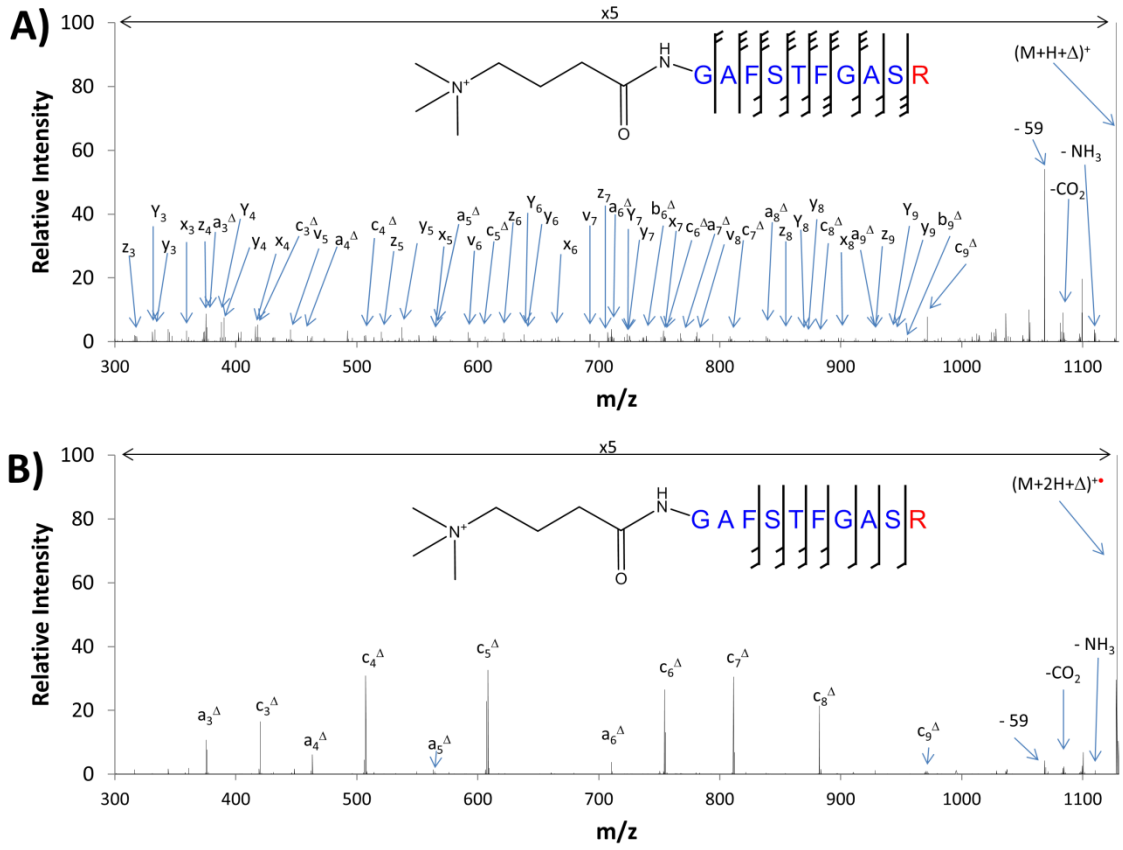

Figure 2.4. A) UVPD of A) +1 ion of N-terminal fixed-charge peptide QA^+-GAFSTFGASR, and B) ETuvPD of charge-reduced species of N-terminal fixed-charge peptide QA^+-GAFSTFGASR showing simplified fragmentation. Δ = ions containing fixed-charge tag.

The analogous CAD and HCD spectra for each of the three singly protonated peptides are shown in **Figures 2.7, 2.8,** and **2.9.** CAD spectra of the peptides that contained an N- or C-terminal arginine (**Figures 2.7A** and **2.8A**) followed previous trends of dominant loss of NH_3 from the protonated arginine sidechain.[28] HCD spectra of those same peptides (**Figures 2.7B and 2.8B**) showed higher conversion efficiencies of precursor to backbone fragment ions. As expected, CAD and HCD of the N-terminal arginine peptide generated N-terminal fragment ions; CAD and HCD of the C-terminal arginine peptide generated a mixture of N- and C-terminal fragments due to the

possibility of two protonation sites (N-terminal amine and Arg). CAD and HCD of GAFSTFGASS produced a mixture of N- and C-terminal fragments (**Figure 2.9**).

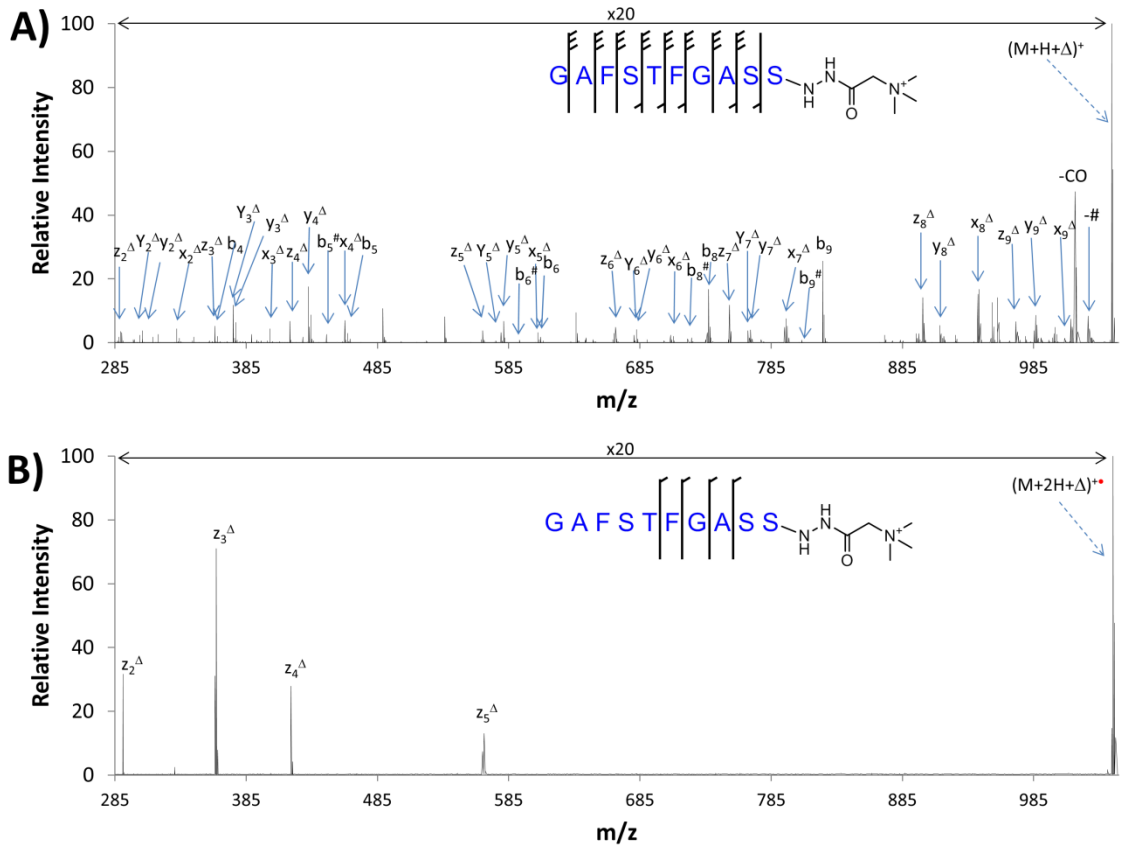

Figure 2.5. A) UVPD of A) +1 ion of C-terminal fixed-charge peptide GAFSTFGASS-QA+, and B) ETuvPD of charge-reduced species of C-terminal fixed-charge peptide GAFSTFGASS-QA+ showing simplified fragmentation. # = water loss, * = ammonia loss, and Δ = ions containing the fixed-charge tag.

The UVPD mass spectra of the corresponding charge-reduced peptides are shown in **Figure 2.2**. In this case, doubly protonated peptides (2+) were subjected to electron transfer reactions to generate charged-reduced species, then the charged-reduced peptides ($1+^{\cdot}$) were subjected to UVPD (in a net hybrid process termed ETuvPD). The fragmentation patterns of the odd electron charge-reduced peptides were generally much

simpler than the patterns of the conventional protonated peptides in terms of the number of fragment ions produced, displaying mainly *c*- and *z*-type ions, ones that are traditionally observed upon electron activation. For all three peptides and their fixed-charge analogs, this spectral simplification was especially true for ETuvPD (in comparison to ETcaD and EThcD) for which the number of different fragment ions typically decreased by ~50% for the charge-reduced peptides.

In this study, we were particularly interested in evaluating the impact of fixed-charge attachment in comparison to conventional protonation on the UVPD behavior of the peptides, in addition to assessing the impact of charge-reduction of the peptides by electron attachment, yielding odd electron peptides. Comparative examples of the UVPD spectra for the resulting peptide ions are shown in **Figures 2.3, 2.4, 2.5** and **Figure 2.10 (**and summarized in **Figure 2.6** and **Table 2.1),** and key results are described in the following sections.

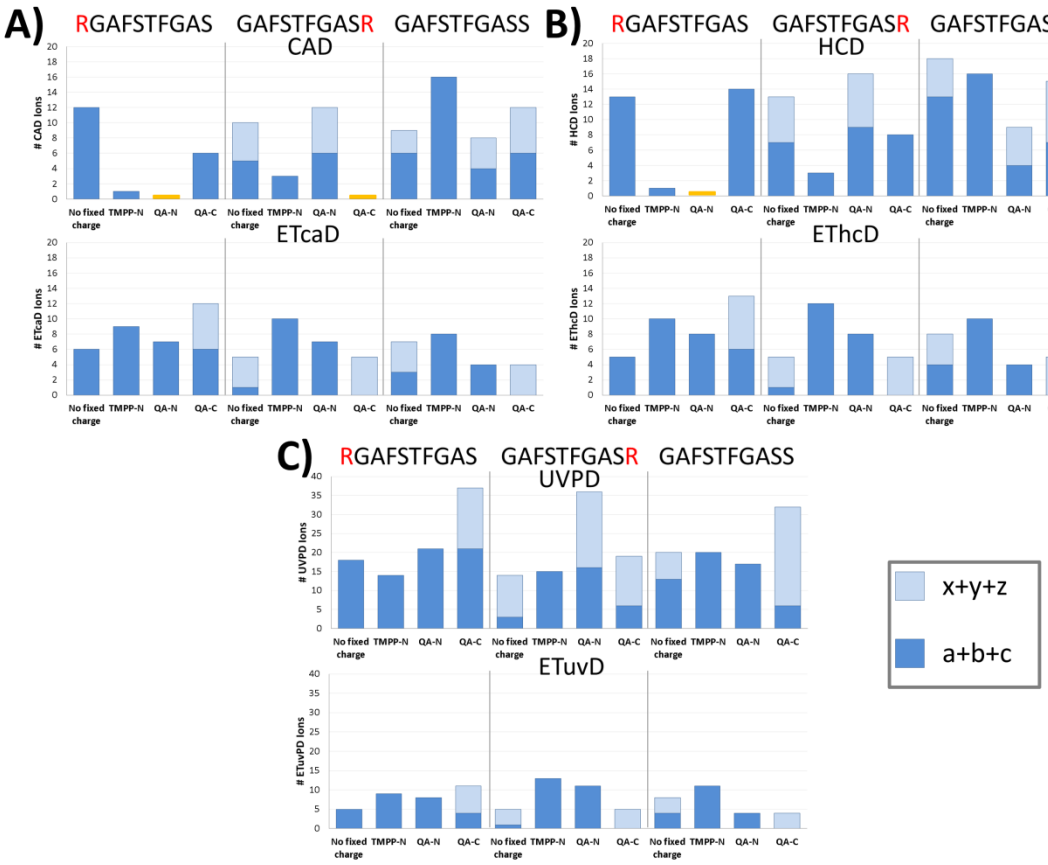

Figure 2.6. Number of fragment ions identified for peptides RGAFSTFGAS, GAFSTFGASR, and GAFSTFGASS with no fixed charge, TMPP N-terminal fixed charge (TMPP-N), quaternary amine N-terminal fixed charge (QA-N), and quaternary amine C-terminal fixed charge (QA-C). A) CAD versus ETcaD, B) HCD versus EThcD, and C) UVPD versus ETuvPD. Light blue bars represent C-terminal (x,y,z) fragment ion types and dark blue bars represent N-terminal (a,b,c) fragment ion types. The gold bars indicate that no fragments were identified. Note that the scale of the y-axis in C is double the scale of A and B.

N-Terminal Arginine (RGAFSTFGAS)

Examples of the UVPD mass spectra for the C-terminal quaternary amine fixed-charged peptide RGAFSTFGAS-QA$^+$ are shown in **Figure 2.3**. This is an interesting peptide since the basic Arg residue at the N-terminus is known to sequester a proton (resulting in the predominance of N-terminal fragment ions observed in **Figure 2.1A**),

whereas the attachment of the fixed-charge quaternary amine at the C-terminus localizes a single charge at the opposite end of the peptide. UVPD of the fixed-charge peptide results in a mixture of N- and C-terminal fragments (**Figure 2.3A**). The unexpected formation of N-terminal product ions in **Figure 2.3A** despite the fixed-charge at the C-terminus is rationalized through the liberation of trimethylamine upon nucleophilic attack by a carbonyl oxygen or an amide nitrogen to re-generate a mobile proton which may migrate to the N-terminal Arg, via a process identical to that reported by Reilly *et al*.[45] The neutral loss of trimethylamine is prominent in the UVPD spectrum (**Figure 2.3A**) of the RGAFSTFGAS-QA$^+$ peptide, as was also dominant in the CAD and HCD spectra (spectra not shown, see **Table 2.1**). UVPD of the corresponding charged-reduced peptide resulted in a substantially simplified spectrum (**Figure 2.3B**), comprised of only *c*- and *z*-type fragment ions which are radical-mediated products commonly observed upon ETD. The *z*-type ions are more abundant than the *c*-type, suggesting greater retention of the charge at the C-terminus, and there is a notable reduction in the loss of trimethylamine that was a dominant process upon UVPD of the even electron fixed-charge peptide (**Figure 2.3A**).

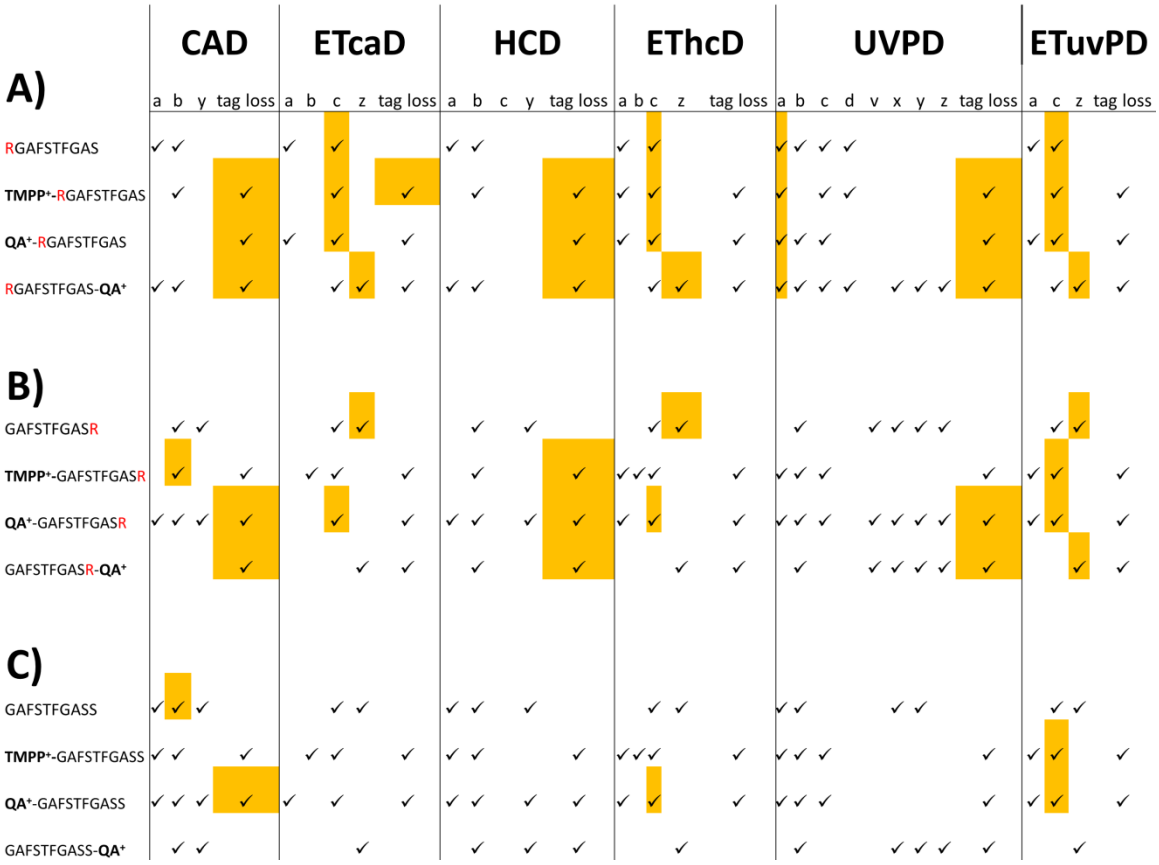

Table 2.1. CAD, ETcaD, HCD, EThcD, UVPD, and ETuvPD identified fragment ions for A) RGAFSTFGAS, B) GAFSTFGASR, and C) GAFSTFGASS peptides as unmodified form, or modified with TMPP at the N-terminal, or modified with a quaternary amine (QA) at the N-terminal or C-terminal. Tag loss means elimination of trimethyl amine for the quaternary amine-derivatized peptides or formation of $TMPP^+$ for the TMPP-modified peptides. The gold shading represents most relative abundant ion types.

Beyond a dominant neutral loss of trimethylamine during collisional activation (CAD and HCD) of singly charged RGAFSTFGAS-QA^+, N-terminal fragment ions were observed at very low relative abundance (**Table 2.1**). These ions may be the result of charge-remote fragmentation (after a proton is relocated to the N-terminal Arg) since HCD resulted in more fragments identified (14) than lower energy CAD (6). Collisional activation of the odd electron, charge-reduced form of RGAFSTFGAS-QA^+ resulted in

less prominent loss of trimethylamine and formation of a distribution of *c*- and *z*-type ions with *z*-type ions being more abundant. This is an interesting result because it reflects a degree of charge mobility that was not observed for the singly protonated or fixed-charge peptide.

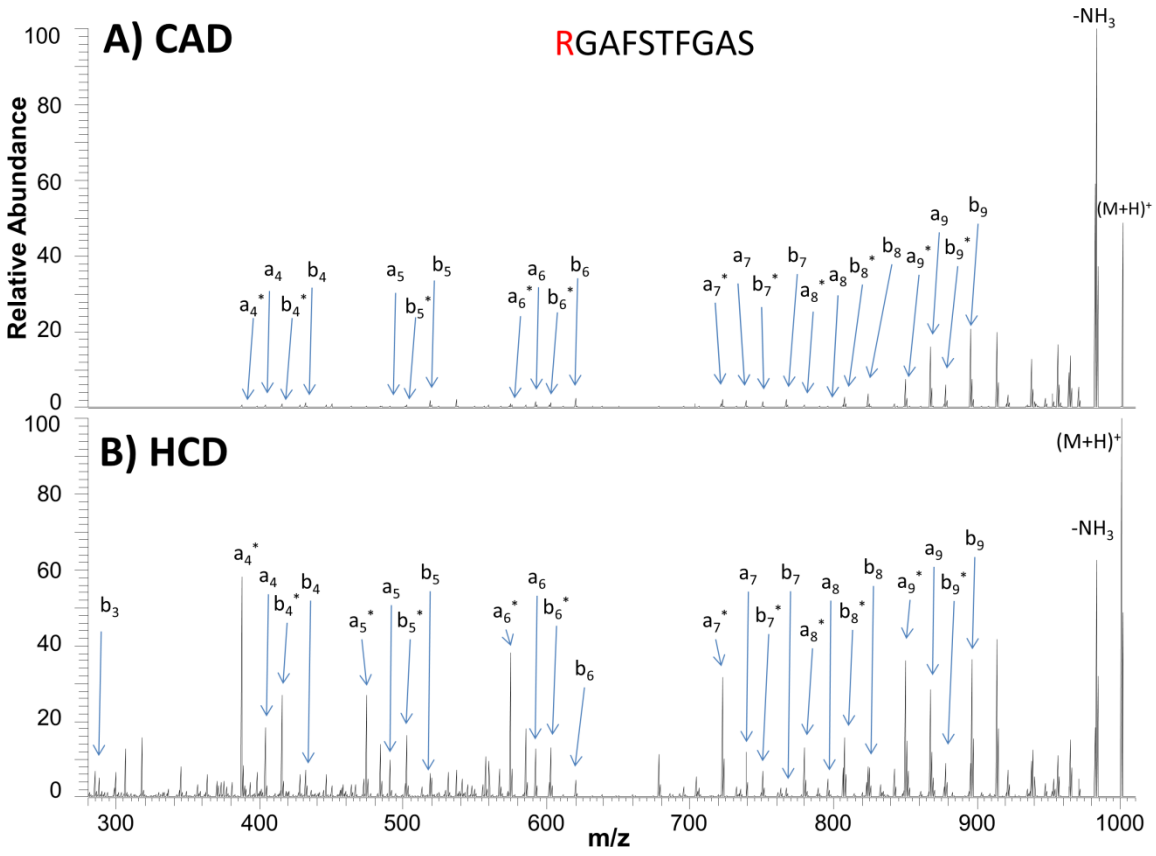

Figure 2.7. MS/MS spectra of protonated RGAFSTFGAS using A) CAD and B) HCD. # = water loss, * = ammonia loss.

Attachment of a quaternary amine tag to the N-terminus of peptide RGAFSFGAS resulted in a fixed-charge peptide (QA^+-RGAFSFGAS) in which the loss of trimethylamine was dominant upon CAD, HCD or UVPD, in addition to production of over 20 N-terminal fragment ions (*a,b,c*) upon UVPD (**Figure 2.6** and **Table 2.1**). The

fact that UVPD was more effective at producing sequence ions than CAD or HCD for the N-terminal modified peptide is attributed to the broader range of UV-activated fragmentation pathways that remain competitive with simple cleavage of trimethylamine. In contrast to the prominent loss of trimethylamine for QA^+-RGAFSFGAS upon CAD or HCD, ETcaD and EThcD (i.e. interrogation of the odd electron peptide created after electron attachment to the protonated fixed-charged peptide) resulted in a series of diagnostic *c* and *z* ions. ETuvPD produced a similar series of *c/z* ions, but the total number of different fragment ions (8 fragment ions) was significantly lower in comparison to UVPD of the even electron fixed-charge peptide (20 fragment ions). This "simplification" of the UVPD spectrum is a recurring theme throughout this study, as also witnessed for the other even electron peptides.

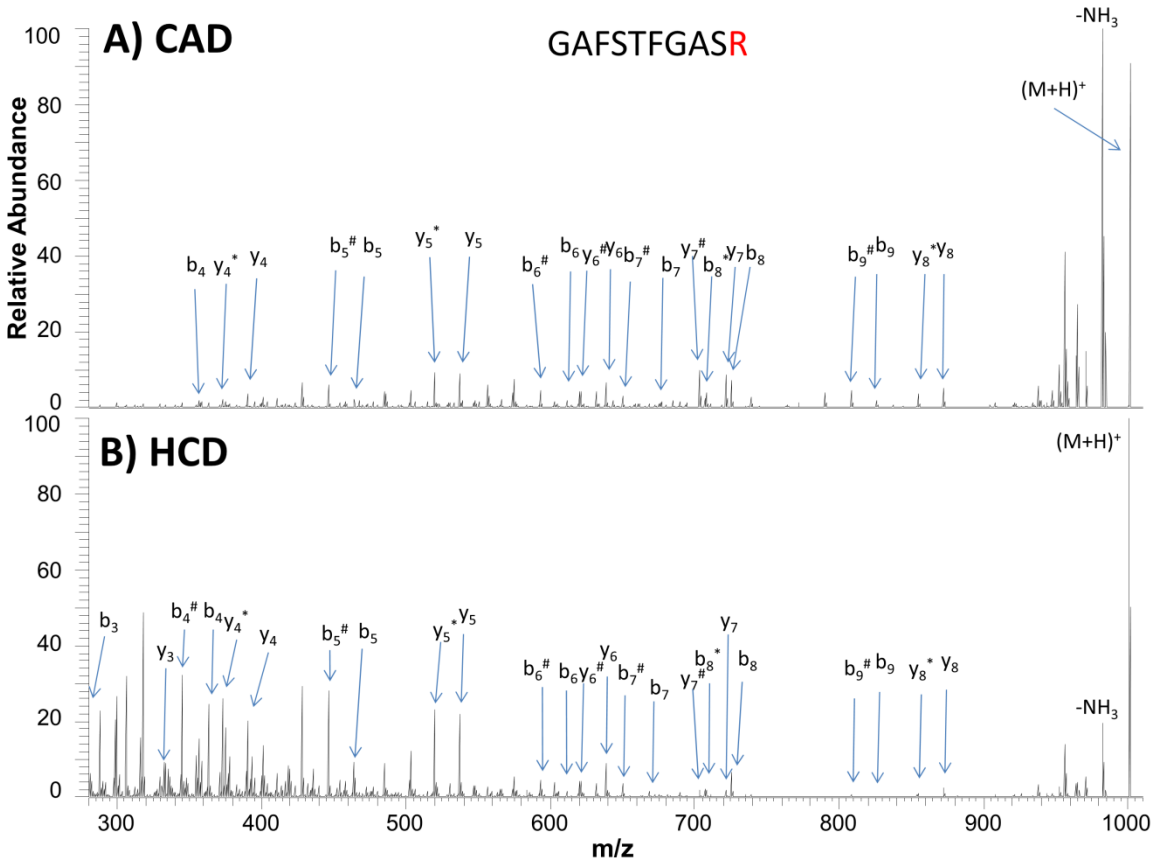

Figure 2.8. MS/MS spectra of protonated GAFSTFGASR using A) CAD and B) HCD. # = water loss, * = ammonia loss.

A second N-terminal fixed-charge peptide was generated by attachment of the TMPP tag to RGAFSTFGAS. Examples of UVPD and ETuvPD mass spectra for the resulting $TMPP^+$- RGAFSTFGAS peptide are shown in **Figure 2.10**, and the CAD, HCD, ETcaD, and EThcD results are summarized in **Figure 2.6** and **Table 2.1**. The even electron fixed-charge peptide dissociated predominantly by the loss of the charged TMPP tag (resulting in the $TMPP^+$ ion of m/z 573) in addition to the formation of some low abundance TMPP-containing N-terminal fragment ions (*a,c,d* ions) (**Figure 2.10A**). UVPD of the corresponding odd electron charge-reduced peptide produced a series of N-terminal *c* ions, giving nearly full sequence coverage, with a significant reduction in the

abundance of the TMPP tag ion (**Figure 2.10B**). The number and types of N-terminal *c* ions produced by ETcaD, EThcD, and ETuvPD for charge-reduced $TMPP^{+}$-RGAFSTFGAS were almost identical for all three hybrid methods (**Figure 2.6**). In general, attachment of the TMPP fixed charge tag to the N-terminus resulted in the exclusive formation of N-terminal fragment ions for all peptides and for all activation methods as well as for both odd and even electron precursors. Thus, the presence of the TMPP fixed charge at the N-terminus had a dramatic and consistent impact on peptide fragmentation.

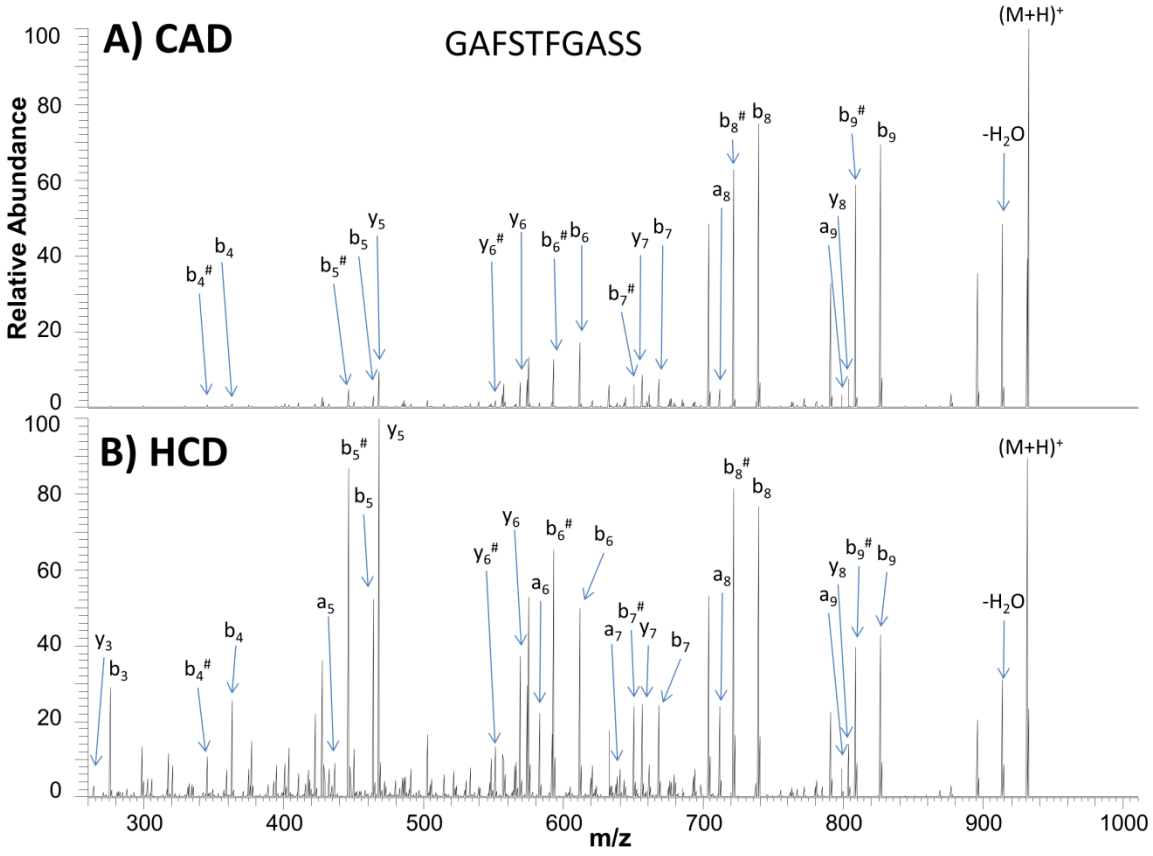

Figure 2.9. MS/MS spectra of protonated GAFSTFGASS using A) CAD and B) HCD. # = water loss, * = ammonia loss.

C-Terminal Arginine (GAFSTFGASR)

The number and types (C-terminal versus N-terminal) of fragment ions produced upon CAD, ETcaD, HCD, EThcD, UVPD, and ETuvPD for protonated GAFSTFGASR and its fixed-charged variants are summarized in **Figure 2.6** and **Table 2.1**. Protonated or charge-reduced GAFSTFGASR produced a mixture of N-terminal and C-terminal fragment ions upon CAD, HCD, or UVPD. Attachment of a quaternary ammonium fixed charge to the N-terminus (QA^+-GAFSTFGASR) led to significant loss of trimethylamine upon UVPD (as noted for other quaternary amine-tagged peptides), as well as formation of an extensive array of N- and C-terminal fragment ions (*a,b,c, x, y, z*) (**Figure 2.4A**). In contrast, UVPD of charge-reduced QA^+-GAFSTFGASR resulted solely in N-terminal product ions: a clean series of *c* ions as well as several *a* ions (**Figure 2.4B**). UVPD of the peptide created by replacement of the quaternary amine tag by the TMPP fixed charge tag at the N-terminus ($TMPP^+$-GAFSTFGASR) yielded only N-terminal fragment ions, supporting the hypothesis that the C-terminal fragment ions produced upon UVPD of QA^+-GAFSTFGASR arise after cleavage of trimethylamine and generation of a mobile proton. The UVPD spectrum of the charge-reduced $TMPP^+$-GAFSTFGASR is very similar to that of QA^+-GAFSTFGASR: showing series of *a* and *c* ions with the latter more abundant than the former.

UVPD of the peptide modified by attachment of a fixed charge to the C-terminus (GAFSTFGASR-QA+) led to the prominent loss of trimethylamine, in addition to low abundances of N- and C-terminal fragment ions (b,x,y,z). In contrast, UVPD of the charge-reduced peptide resulted solely in production of C-terminal z ions, similar to those observed upon CAD or HCD of the same charge-reduced peptide.

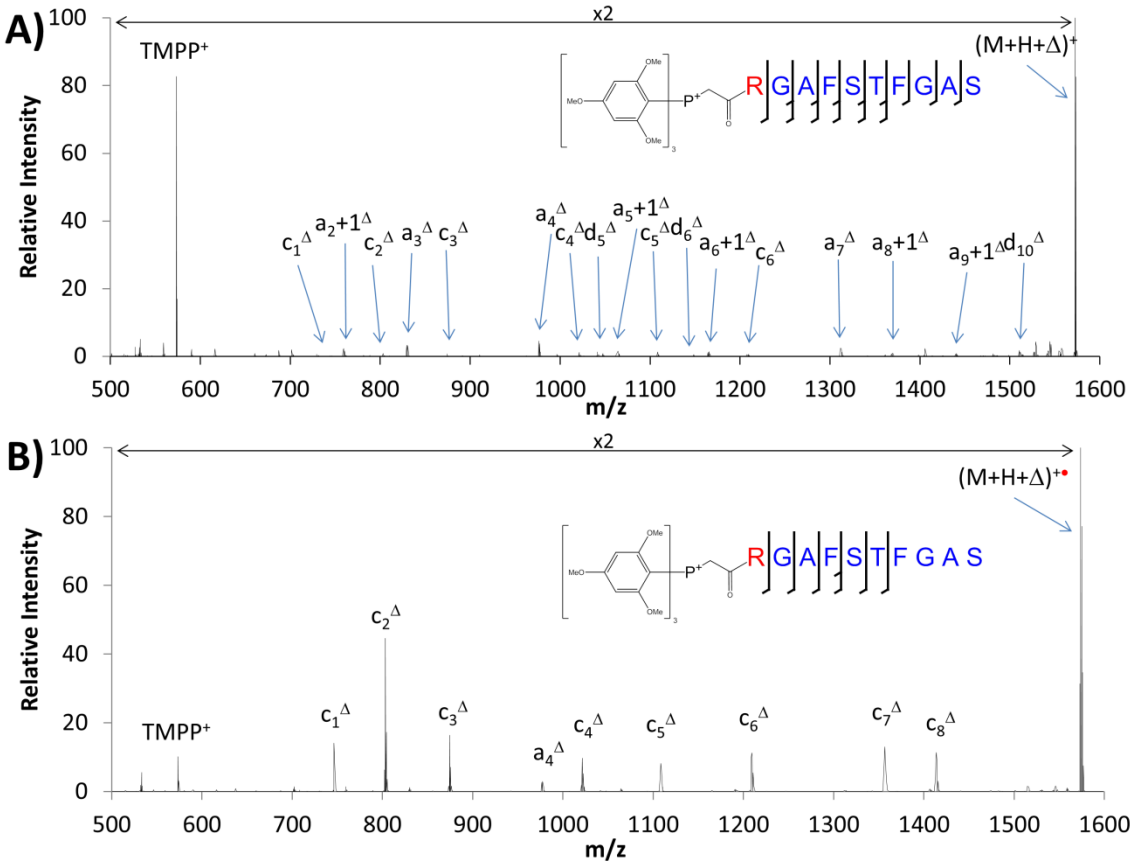

Figure 2.10. A) UVPD of N-terminal fixed-charge peptide TMPP-RGAFSTFGAS showing a dominant tag loss. B) ETuvPD of charge-reduced N-terminal fixed-charge peptide TMPP-RGAFSTFGAS showing reduction in the prominence of the tag loss and simplified fragmentation. Δ = containing fixed charge tag.

No Arginine (GAFSTFGASS)

A final peptide containing no amino acids with basic side-chains, GAFSTFGASS, was evaluated. Upon UVPD of the protonated or charge-reduced peptide, both N- and C-terminal ions were produced; *a,b*, and *x,y* for the protonated peptide and *c* and *z* for the charge-reduced peptide. This latter outcome again mirrors the observation that dissociation of peptides that are charge-reduced exclusively occurs via the electron-mediated pathways common to ETD, not the more diverse pathways commonly observed

upon UVPD of protonated peptides. Modification of the peptide by attachment of a quaternary ammonium fixed charge to the N-terminus (QA^+-GAFSTFGASS) again yielded a prominent loss of trimethylamine upon UVPD, in addition to a substantial series of N-terminal fragment ions (*a,b,c,*), a result consistent with sequestration of the charge site at the N-terminus. UVPD of charge-reduced QA^+-GAFSTFGASS likewise resulted solely in N-terminal product ions; however in this case only *a* and *c* ions, no *b* ions, were formed, and the number of different fragment ions was reduced by a factor of three compared to UVPD of even electron QA^+-GAFSTFGASS.

UVPD of the fixed-charge peptide produced by substitution of the quaternary amine tag by the TMPP tag at the N-terminus ($TMPP^+$-GAFSTFGASS) yielded nearly an identical series of fragment ions as observed upon UVPD of QA^+-GAFSTFGASS. ETuvPD (analysis of the charge-reduced peptide) also resulted in nearly identical fragmentation patterns for QA^+-GAFSTFGASS and $TMPP^+$-GAFSTFGASS. **Figure 2.5** shows the UVPD spectra obtained for GAFSTFGASS-QA^+ (quaternary amine appended to the C-terminus). Similar to UVPD of the unmodified peptide, both C-terminal and N-terminal fragments were produced for the even electron fixed-charge peptide (**Figure 2.5A)**, suggesting that the production of the *a,b,c,x,y,* and *z* ions occurred in a manner that was not modulated by a mobile proton. In contrast, ETuvPD of the charge-reduced GAFSTFGASS-QA^+ peptide resulted solely in a clean series of C-terminal *z* ions in a manner consistent with radical-mediated pathways (**Figure 2.5B**).

For RGAFSTFGAS, N-terminal fragments were always favored for the unmodified peptide and for both types of N-terminal modified peptides (TMPP and QA), whether activated as even-electron or charge-reduced odd electron species. However, for RGAFSTFGAS with a fixed charge (QA) at the C-terminus, both C- and N-terminal ions were observed for the charge-reduced peptides upon ETcaD, EThcD, UVPD, and

ETuvPD. For GAFSTFGASR and GAFSTFGASS, there was greater variation in whether C- or N-terminal fragments or both types were formed, and the outcome depended on the activation method (CAD, HCD versus UVPD). The unmodified peptides give a mixture of C- and N-terminal fragments by CAD, HCD, and UVPD. Modification of these two peptides by attachment of TMPP at the N-terminus resulted solely in formation of N-terminal fragment ions, confirming the dominant role of the fixed charge on the fragmentation behavior. In contrast, addition of a quaternary amine at the N-terminus of GAFSTFGASR and GAFSTFGASS led to formation of both C- and N-terminal ions, but yielded only N-terminal ions for the charge-reduced peptides. Unlike the TMPP tag, the quaternary amine tag underwent cleavage to eliminate trimethyl amine and generate a mobile proton that facilitated formation of the unexpected C- or N-terminal ions upon CAD and HCD despite the location of a charge-sequestering Arg residue. However, the N-terminal quaternary amine-tagged GAFSTFGASR and GAFSTFGASS peptides yielded only N-terminal ions for the charge-reduced species, cleavage of trimethyl amine was no longer dominant, and the resulting fragment ions were dictated by radical-mediated pathways.

One of the most notable findings from the collection of results for the three peptides in the fixed-charge forms was the similarities of the fragmentation patterns, both in terms of number and types of fragment ions, obtained upon CAD, HCD and UVPD of the charge-reduced species (i.e. odd electron peptides). This result contrasted with the substantially greater diversity of fragment ions produced by UVPD relative to CAD and HCD for the protonated and fixed-charge peptides. Reference ETD spectra collected for the doubly-charged peptides (those with one proton and one fixed charge site) resulted in the production of *c* or *z* fragment ions depending on the location of the fixed charge site. Activation of charge-reduced peptide ions, whether by collisions or photons, led to the

same *c* and or *z* ions observed upon ETD, thus recapitulating the dominance of the radical-mediated pathways regardless of activation method

CONCLUSIONS 2.5

The influence of four key factors on the fragmentation patterns of peptides has been examined: i) location of a basic site (Arg), ii) impact of a fixed charge, iii) conversion of conventional even electron peptides to odd electron peptides, and iv) activation method (collisional versus photoactivation). The two charge tags appended to the N-terminus (TMPP and QA) modulated the fragmentation pathways in different ways, with the TMPP acting as a true fixed charge site and leading to dominant and exclusive formation of N-terminal fragment ions, whereas the quaternary amine underwent cleavage to release a mobile proton in a manner noted previously by Reilly *et al*.[45,50] The generation of a mobilized proton occurred for those peptides modified with a quaternary amine at the C- or N-terminus. For all peptides, whether containing a fixed charge site or not and whether containing a basic Arg residue or not, the fragmentation patterns of the charge-reduced species (those created via electron transfer as the first activation step) resulted in clean production of *c* and *z* ions upon secondary activation of CAD, HCD, or UVPD, and the resulting hybrid activation spectra were remarkably similar for ETcaD, EThcD, and ETuvPD despite the well-known differences in the collisional activation and photoactivation processes. Although UVPD is well known to create rich fragmentation patterns for protonated peptides, this was not the case for UVPD of odd electron peptides, and instead the resulting spectra were much simpler than typical UVPD mass spectra and nearly identical to the spectra produced by ETD (*c/z* ions). The dominance of the radical-mediated fragmentation pathways underscored the overwhelming impact of the radical site, more-so than the presence of a fixed charge or

the type of activation method used. From a practical standpoint, this outcome suggests a strategy for simplifying overly congested MS/MS spectra (particularly UVPD spectra) by incorporating an initial charge-reduction step to consolidate fragmentation into *c/z* ions.

References

1 R.A. Zubarev, N.L. Kelleher, F.W. McLafferty, Electron Capture Dissociation of Multiply Charged Protein Cations. A Nonergodic Process, Journal of the American Chemical Society. 120 (1998) 3265–3266. doi:10.1021/ja973478k.

2 J.E.P. Syka, J.J. Coon, M.J. Schroeder, J. Shabanowitz, D.F. Hunt, Peptide and protein sequence analysis by electron transfer dissociation mass spectrometry, Proceedings of the National Academy of Sciences of the United States of America. 101 (2004) 9528–9533. doi:10.1073/pnas.0402700101.

3 X. Li, X. Yu, C.E. Costello, C. Lin, P.B. O'Connor, Top-Down Study of β_2-Microglobulin Deamidation, Analytical Chemistry. 84 (2012) 6150–6157. doi:10.1021/ac3009324.

4 C.K. Frese, A.F.M. Altelaar, H. van den Toorn, D. Nolting, J. Griep-Raming, A.J.R. Heck, et al., Toward Full Peptide Sequence Coverage by Dual Fragmentation Combining Electron-Transfer and Higher-Energy Collision Dissociation Tandem Mass Spectrometry, Analytical Chemistry. 84 (2012) 9668–9673. doi:10.1021/ac3025366.

5 C.K. Frese, H. Zhou, T. Taus, A.F.M. Altelaar, K. Mechtler, A.J.R. Heck, et al., Unambiguous Phosphosite Localization using Electron-Transfer/Higher-Energy Collision Dissociation (EThcD), Journal of Proteome Research. 12 (2013) 1520–1525. doi:10.1021/pr301130k.

6 S.I. Smith, J.S. Brodbelt, Hybrid Activation Methods for Elucidating Nucleic Acid Modifications, Analytical Chemistry. 83 (2011) 303–310. doi:10.1021/ac102411a.

7 J.A. Madsen, R.R. Cheng, T.S. Kaoud, K.N. Dalby, D.E. Makarov, J.S. Brodbelt, Charge-Site-Dependent Dissociation of Hydrogen-Rich Radical Peptide Cations upon Vacuum UV Photoexcitation, Chemistry - A European Journal. 18 (2012) 5374–5383. doi:10.1002/chem.201103534.

8 J.B. Shaw, W. Li, D.D. Holden, Y. Zhang, J. Griep-Raming, R.T. Fellers, et al., Complete Protein Characterization Using Top-Down Mass Spectrometry and Ultraviolet Photodissociation, J. Am. Chem. Soc. 135 (2013) 12646–12651. doi:10.1021/ja4029654.

9 J.R. Cannon, C. Kluwe, A. Ellington, J.S. Brodbelt, Characterization of green fluorescent proteins by 193 nm ultraviolet photodissociation mass spectrometry, PROTEOMICS. 14 (2014) 1165–1173. doi:10.1002/pmic.201300364.

10 J.R. Cannon, M.B. Cammarata, S.A. Robotham, V.C. Cotham, J.B. Shaw, R.T. Fellers, et al., Ultraviolet Photodissociation for Characterization of Whole Proteins on a Chromatographic Time Scale, Analytical Chemistry. 86 (2014) 2185–2192. doi:10.1021/ac403859a.

11 C.K. Frese, D. Nolting, A.F.M. Altelaar, J. Griep-Raming, S. Mohammed, A.J.R. Heck, Characterization of Electron Transfer Dissociation in the Orbitrap Velos HCD Cell, Journal of The American Society for Mass Spectrometry. 24 (2013) 1663–1670. doi:10.1007/s13361-013-0618-9.

12 L.A. Vasicek, A.R. Ledvina, J. Shaw, J. Griep-Raming, M.S. Westphall, J.J. Coon, et al., Implementing Photodissociation in an Orbitrap Mass Spectrometer, Journal of The American Society for Mass Spectrometry. 22 (2011) 1105–1108. doi:10.1007/s13361-011-0119-7.

13 D.M. Good, M. Wirtala, G.C. McAlister, J.J. Coon, Performance characteristics of electron transfer dissociation mass spectrometry, Mol. Cell Proteomics. 6 (2007) 1942–1951. doi:10.1074/mcp.M700073-MCP200.

14 S.J. Hardy, C.G. Kurland, P. Voynow, G. Mora, The ribosomal proteins of Escherichia coli. I. Purification of the 30S ribosomal proteins, Biochemistry. 8 (1969) 2897–2905.

15 J. Cannon, K. Lohnes, C. Wynne, Y. Wang, N. Edwards, C. Fenselau, High-Throughput Middle-Down Analysis Using an Orbitrap, Journal of Proteome Research. 9 (2010) 3886–3890. doi:10.1021/pr1000994.

16 S.-L. Wu, A.F.R. Hühmer, Z. Hao, B.L. Karger, On-line LC-MS approach combining collision-induced dissociation (CID), electron-transfer dissociation (ETD), and CID of an isolated charge-reduced species for the trace-level characterization of proteins with post-translational modifications, J. Proteome Res. 6 (2007) 4230–4244. doi:10.1021/pr070313u.

17 D.M. Horn, Y. Ge, F.W. McLafferty, Activated Ion Electron Capture Dissociation for Mass Spectral Sequencing of Larger (42 kDa) Proteins, Analytical Chemistry. 72 (2000) 4778–4784. doi:10.1021/ac000494i.

18 A.R. Ledvina, N.A. Beauchene, G.C. McAlister, J.E.P. Syka, J.C. Schwartz, J. Griep-Raming, et al., Activated-Ion Electron Transfer Dissociation Improves the Ability of Electron Transfer Dissociation to Identify Peptides in a Complex Mixture, Analytical Chemistry. 82 (2010) 10068–10074. doi:10.1021/ac1020358.

19 N. Taouatas, M.M. Drugan, A.J.R. Heck, S. Mohammed, Straightforward ladder sequencing of peptides using a Lys-N metalloendopeptidase, Nature Methods. 5 (2008) 405–407. doi:10.1038/nmeth.1204.

20 A.R. Ledvina, G.C. McAlister, M.W. Gardner, S.I. Smith, J.A. Madsen, J.C. Schwartz, et al., Infrared Photoactivation Reduces Peptide Folding and Hydrogen-Atom Migration following ETD Tandem Mass Spectrometry, Angewandte Chemie International Edition. 48 (2009) 8526–8528. doi:10.1002/anie.200903557.

21 J.S. Cobb, M.L. Easterling, J.N. Agar, Structural characterization of intact proteins is enhanced by prevalent fragmentation pathways rarely observed for peptides, Journal of the American Society for Mass Spectrometry. 21 (2010) 949–959. doi:10.1016/j.jasms.2010.02.009.

22 T.E. Angel, U.K. Aryal, S.M. Hengel, E.S. Baker, R.T. Kelly, E.W. Robinson, et al., Mass spectrometry-based proteomics: existing capabilities and future directions, Chemical Society Reviews. 41 (2012) 3912. doi:10.1039/c2cs15331a.

23 Y. Zhang, B.R. Fonslow, B. Shan, M.-C. Baek, J.R. Yates, Protein Analysis by Shotgun/Bottom-up Proteomics, Chemical Reviews. 113 (2013) 2343–2394. doi:10.1021/cr3003533.

24 T.C. Walther, M. Mann, Mass spectrometry-based proteomics in cell biology, The Journal of Cell Biology. 190 (2010) 491–500. doi:10.1083/jcb.201004052.

25 F. Schütz, E.A. Kapp, R.J. Simpson, T.P. Speed, Deriving statistical models for predicting peptide tandem MS product ion intensities, Biochem. Soc. Trans. 31 (2003) 1479–1483. doi:10.1042/.

26 V.H. Wysocki, G. Tsaprailis, L.L. Smith, L.A. Breci, Mobile and localized protons: a framework for understanding peptide dissociation, Journal of Mass Spectrometry. 35 (2000) 1399–1406. doi:10.1002/1096-9888(200012)35:12<1399::AID-JMS86>3.0.CO;2-R.

27 L.A. Breci, D.L. Tabb, J.R. Yates, V.H. Wysocki, Cleavage N-terminal to proline: analysis of a database of peptide tandem mass spectra, Anal. Chem. 75 (2003) 1963–1971. doi:10.1021/ac026359i.

28 A.R. Dongré, J.L. Jones, Á. Somogyi, V.H. Wysocki, Influence of Peptide Composition, Gas-Phase Basicity, and Chemical Modification on Fragmentation Efficiency: Evidence for the Mobile Proton Model, J. Am. Chem. Soc. 118 (1996) 8365–8374. doi:10.1021/ja9542193.

29 H. Steen, M. Mann, The abc's (and xyz's) of peptide sequencing, Nature Reviews Molecular Cell Biology. 5 (2004) 699–711. doi:10.1038/nrm1468.

30 A.G. Sullivan, F.L. Brancia, R. Tyldesley, R. Bateman, K. Sidhu, S.J. Hubbard, et al., The exploitation of selective cleavage of singly protonated peptide ions adjacent to aspartic acid residues using a quadrupole orthogonal time-of-flight mass spectrometer equipped with a matrix-assisted laser desorption/ionization source, International Journal of Mass Spectrometry. 210-211 (2001) 665–676. doi:10.1016/S1387-3806(01)00430-4.

31 F. Kjeldsen, A.M.B. Giessing, C.R. Ingrell, O.N. Jensen, Peptide sequencing and characterization of post-translational modifications by enhanced ion-charging and liquid chromatography electron-transfer dissociation tandem mass spectrometry, Anal. Chem. 79 (2007) 9243–9252. doi:10.1021/ac701700g.

32 B.L. Frey, C.J. Krusemark, A.R. Ledvina, J.J. Coon, P.J. Belshaw, L.M. Smith, Ion-Ion Reactions with Fixed-Charge Modified Proteins to Produce Ions in a Single, Very High Charge State, Int J Mass Spectrom. 276 (2008) 136–143. doi:10.1016/j.ijms.2008.07.029.

33 C. Krusemark, B. Frey, P. Belshaw, L. Smith, Modifying the charge state distribution of proteins in electrospray ionization mass spectrometry by chemical derivatization, J Am Soc Mass Spectrom. 20 (2009) 1617–1625. doi:10.1016/j.jasms.2009.04.017.

34 X. Li, J. Cournoyer, C. Lin, P. Oconnor, The Effect of Fixed Charge Modifications on Electron Capture Dissociation, Journal of the American Society for Mass Spectrometry. 19 (2008) 1514–1526. doi:10.1016/j.jasms.2008.06.014.

35 J. Chamot-Rooke, G. van der Rest, A. Dalleu, S. Bay, J. Lemoine, The combination of electron capture dissociation and fixed charge derivatization increases sequence coverage for O-glycosylated and O-phosphorylated peptides, J. Am. Soc. Mass Spectrom. 18 (2007) 1405–1413. doi:10.1016/j.jasms.2007.04.008.

36 B.M. Ueberheide, D. Fenyo, P.F. Alewood, B.T. Chait, Rapid sensitive analysis of cysteine rich peptide venom components, Proceedings of the National Academy of Sciences. 106 (2009) 6910–6915. doi:10.1073/pnas.0900745106.

37 H.P. Gunawardena, L. Gorenstein, D.E. Erickson, Y. Xia, S.A. McLuckey, Electron transfer dissociation of multiply protonated and fixed charge disulfide linked polypeptides, International Journal of Mass Spectrometry. 265 (2007) 130–138. doi:10.1016/j.ijms.2007.01.017.

38 L. Zhang, Y. Xu, H. Lu, P. Yang, Carboxy group derivatization for enhanced electron-transfer dissociation mass spectrometric analysis of phosphopeptides, PROTEOMICS. 9 (2009) 4093–4097. doi:10.1002/pmic.200800963.

39 L. Vasicek, J.S. Brodbelt, Enhanced Electron Transfer Dissociation through Fixed Charge Derivatization of Cysteines, Analytical Chemistry. 81 (2009) 7876–7884. doi:10.1021/ac901482s.

40 Y. Lu, X. Zhou, P.M. Stemmer, G.E. Reid, Sulfonium Ion Derivatization, Isobaric Stable Isotope Labeling and Data Dependent CID- and ETD-MS/MS for Enhanced Phosphopeptide Quantitation, Identification and Phosphorylation Site Characterization, Journal of The American Society for Mass Spectrometry. 23 (2012) 577–593. doi:10.1007/s13361-011-0190-0.

41 T.W. Chung, C.L. Moss, M. Zimnicka, R.S. Johnson, R.L. Moritz, F. Tureček, Electron-Capture and -Transfer Dissociation of Peptides Tagged with Tunable Fixed-Charge Groups: Structures and Dissociation Energetics, Journal of The American Society for Mass Spectrometry. 22 (2011) 13–30. doi:10.1007/s13361-010-0012-9.

42 T.W. Chung, F. Tureček, Selecting fixed-charge groups for electron-based peptide dissociations, International Journal of Mass Spectrometry. 276 (2008) 127–135. doi:10.1016/j.ijms.2008.04.014.

43 M. Zimnicka, C. Moss, T. Chung, R. Hui, F. Tureček, Tunable Charge Tags for Electron-Based Methods of Peptide Sequencing: Design and Applications, Journal of The American Society for Mass Spectrometry. 23 (2012) 608–620. doi:10.1007/s13361-011-0184-y.

44 Y. Xu, L. Zhang, H. Lu, P. Yang, Mass Spectrometry Analysis of Phosphopeptides after Peptide Carboxy Group Derivatization, Anal. Chem. 80 (2008) 8324–8328. doi:10.1021/ac801220c.

45 Y. He, J.P. Reilly, Does a Charge Tag Really Provide a Fixed Charge?, Angewandte Chemie International Edition. 47 (2008) 2463–2465. doi:10.1002/anie.200705048.

46 P.-C. Liao, Z.-H. Huang, J. Allison, Charge remote fragmentation of peptides following attachment of a fixed positive charge: A matrix-assisted laser desorption/ionization postsource decay study, Journal of the American Society for Mass Spectrometry. 8 (1997) 501–509. doi:10.1016/S1044-0305(97)81513-9.

47 N. Sadagopan, J.T. Watson, Investigation of the tris(trimethoxyphenyl)phosphonium acetyl charged derivatives of peptides by electrospray ionization mass spectrometry and tandem mass spectrometry, Journal of the American Society for Mass Spectrometry. 11 (2000) 107–119. doi:10.1016/S1044-0305(99)00127-0.

48 N. Sadagopan, J.T. Watson, Mass spectrometric evidence for mechanisms of fragmentation of charge-derivatized peptides, Journal of the American Society for Mass Spectrometry. 12 (2001) 399–409. doi:10.1016/S1044-0305(01)00211-2.

49 P.-C. Liao, Z.-H. Huang, J. Allison, Charge remote fragmentation of peptides following attachment of a fixed positive charge: A matrix-assisted laser desorption/ionization postsource decay study, Journal of the American Society for Mass Spectrometry. 8 (1997) 501–509. doi:10.1016/S1044-0305(97)81513-9.

50 Y. He, R. Parthasarathi, K. Raghavachari, J.P. Reilly, Photodissociation of Charge Tagged Peptides, Journal of The American Society for Mass Spectrometry. 23 (2012) 1182–1190. doi:10.1007/s13361-012-0379-x.

51 C. Morano, X. Zhang, L.D. Fricker, Multiple Isotopic Labels for Quantitative Mass Spectrometry, Analytical Chemistry. 80 (2008) 9298–9309. doi:10.1021/ac801654h.

52 B.J. Ko, J.S. Brodbelt, Enhanced Electron Transfer Dissociation of Peptides Modified at C-terminus with Fixed Charges, Journal of The American Society for Mass Spectrometry. 23 (2012) 1991–2000. doi:10.1007/s13361-012-0458-z.

53 J.A. Madsen, J.S. Brodbelt, Simplifying Fragmentation Patterns of Multiply Charged Peptides by N-Terminal Derivatization and Electron Transfer Collision Activated Dissociation, Analytical Chemistry. 81 (2009) 3645–3653. doi:10.1021/ac9000942.

54 P.-C. Liao, J. Allison, Enhanced detection of peptides in matrix-assisted laser desorption/ionization mass spectrometry through the use of charge-localized derivatives, Journal of Mass Spectrometry. 30 (1995) 511–512. doi:10.1002/jms.1190300318.

55 K.V. Wasslen, L.H. Tan, J.M. Manthorpe, J.C. Smith, Trimethylation Enhancement using Diazomethane (TrEnDi): Rapid On-Column Quaternization of Peptide Amino Groups via Reaction with Diazomethane Significantly Enhances Sensitivity in Mass Spectrometry Analyses via a Fixed, Permanent Positive Charge, Analytical Chemistry. 86 (2014) 3291–3299. doi:10.1021/ac403349c.

56 F.W. McLafferty, D.M. Horn, K. Breuker, Y. Ge, M.A. Lewis, B. Cerda, et al., Electron capture dissociation of gaseous multiply charged ions by Fourier-transform ion cyclotron resonance, Journal of the American Society for Mass Spectrometry. 12 (2001) 245–249. doi:10.1016/S1044-0305(00)00223-3.

57 S.A. McLuckey, J.L. Stephenson, Ion/ion chemistry of high-mass multiply charged ions, Mass Spectrometry Reviews. 17 (1998) 369–407. doi:10.1002/(SICI)1098-2787(1998)17:6<369::AID-MAS1>3.0.CO;2-J.

58 qD.L. Swaney, G.C. McAlister, M. Wirtala, J.C. Schwartz, J.E.P. Syka, J.J. Coon, Supplemental Activation Method for High-Efficiency Electron-Transfer Dissociation of Doubly Protonated Peptide Precursors, Analytical Chemistry. 79 (2007) 477–485. doi:10.1021/ac061457f.

59 A.T. Iavarone, J.C. Jurchen, E.R. Williams, Supercharged Protein and Peptide Ions Formed by Electrospray Ionization, Analytical Chemistry. 73 (2001) 1455–1460. doi:10.1021/ac001251t.

60 A.T. Iavarone, E.R. Williams, Supercharging in electrospray ionization: effects on signal and charge, International Journal of Mass Spectrometry. 219 (2002) 63–72. doi:10.1016/S1387-3806(02)00587-0.

61 A.T. Iavarone, E.R. Williams, Collisionally activated dissociation of supercharged proteins formed by electrospray ionization, Anal. Chem. 75 (2003) 4525–4533.

62 J.R. Cannon, D.D. Holden, J.S. Brodbelt, Hybridizing Ultraviolet Photodissociation with Electron Transfer Dissociation for Intact Protein Characterization, Analytical Chemistry. 86 (2014) 10970–10977. doi:10.1021/ac5036082.

63 A.R. Ledvina, C.M. Rose, G.C. McAlister, J.E.P. Syka, M.S. Westphall, J. Griep-Raming, et al., Activated Ion ETD Performed in a Modified Collision Cell on a Hybrid QLT-Oribtrap Mass Spectrometer, Journal of The American Society for Mass Spectrometry. 24 (2013) 1623–1633. doi:10.1007/s13361-013-0621-1.

64 A.M. Brunner, P. Lössl, F. Liu, R. Huguet, C. Mullen, M. Yamashita, et al., Benchmarking Multiple Fragmentation Methods on an Orbitrap Fusion for Top-down Phospho-Proteoform Characterization, Analytical Chemistry. (2015) 150408105516003. doi:10.1021/acs.analchem.5b00162.

65 C.J. Shaffer, A. Marek, R. Pepin, K. Slovakova, F. Turecek, Combining UV photodissociation with electron transfer for peptide structure analysis: ETD photodissociation, Journal of Mass Spectrometry. 50 (2015) 470–475. doi:10.1002/jms.3551.

66 H.T.H. Nguyen, C.J. Shaffer, A.R. Ledvina, J.J. Coon, F. Tureček, Serine effects on collision-induced dissociation and photodissociation of peptide cation radicals of the z+●-type, International Journal of Mass Spectrometry. 378 (2015) 20–30. doi:10.1016/j.ijms.2014.06.028.

67 H.T.H. Nguyen, C.J. Shaffer, F. Tureček, Probing Peptide Cation–Radicals by Near-UV Photodissociation in the Gas Phase. Structure Elucidation of Histidine Radical Chromophores Formed by Electron Transfer Reduction, The Journal of Physical Chemistry B. 119 (2015) 3948–3961. doi:10.1021/jp511717c.

68 J.A. Madsen, D.R. Boutz, J.S. Brodbelt, Ultrafast Ultraviolet Photodissociation at 193 nm and its Applicability to Proteomic Workflows, Journal of Proteome Research. 9 (2010) 4205–4214. doi:10.1021/pr100515x.

69 M. Cammarata, K.-Y. Lin, J. Pruet, H. Liu, J. Brodbelt, Probing the Unfolding of Myoglobin and Domain C of PARP-1 with Covalent Labeling and Top-Down Ultraviolet Photodissociation Mass Spectrometry, Analytical Chemistry. 86 (2014) 2534–2542. doi:10.1021/ac4036235.

70 J.R. Cannon, C. Kluwe, A. Ellington, J.S. Brodbelt, Characterization of green fluorescent proteins by 193 nm ultraviolet photodissociation mass spectrometry, PROTEOMICS. 14 (2014) 1165–1173. doi:10.1002/pmic.201300364.

71 S. Warnke, C. Baldauf, M.T. Bowers, K. Pagel, G. von Helden, Photodissociation of Conformer-Selected Ubiquitin Ions Reveals Site-Specific *Cis* / *Trans* Isomerization of Proline Peptide Bonds, Journal of the American Chemical Society. 136 (2014) 10308–10314. doi:10.1021/ja502994b.

72 M.B. Cammarata, J.S. Brodbelt, Structural characterization of holo- and apo-myoglobin in the gas phase by ultraviolet photodissociation mass spectrometry, Chem. Sci. 6 (2015) 1324–1333. doi:10.1039/C4SC03200D.

73 J.R. Cannon, K. Martinez-Fonts, S.A. Robotham, A. Matouschek, J.S. Brodbelt, Top-Down 193-nm Ultraviolet Photodissociation Mass Spectrometry for Simultaneous Determination of Polyubiquitin Chain Length and Topology, Analytical Chemistry. 87 (2015) 1812–1820. doi:10.1021/ac5038363.

74 N. Webber, Y. He, J.P. Reilly, 157 nm Photodissociation of Dipeptide Ions Containing N-Terminal Arginine, Journal of The American Society for Mass Spectrometry. 25 (2014) 196–203. doi:10.1007/s13361-013-0762-2.

75 L. Zhang, J.P. Reilly, Peptide Photodissociation with 157 nm Light in a Commercial Tandem Time-of-Flight Mass Spectrometer, Anal. Chem. 81 (2009) 7829–7838. doi:10.1021/ac9012557.

76 T.-Y. Kim, J.P. Reilly, Time-resolved observation of product ions generated by 157 nm photodissociation of singly protonated phosphopeptides, J. Am. Soc. Mass Spectrom. 20 (2009) 2334–2341. doi:10.1016/j.jasms.2009.08.021.

77 S.H. Yoon, J.H. Moon, M.S. Kim, Dissociation mechanisms and implication for the presence of multiple conformations for peptide ions with arginine at the C-terminus: time-resolved photodissociation study, Journal of Mass Spectrometry. 45 (2010) 806–814. doi:10.1002/jms.1773.

78 S.H. Yoon, J.H. Moon, Y.J. Chung, M.S. Kim, Influence of basic residues on dissociation kinetics and dynamics of singly protonated peptides: time-resolved photodissociation study, Journal of Mass Spectrometry. 44 (2009) 1532–1537. doi:10.1002/jms.1670.

79 J.H. Moon, Y.S. Shin, H.J. Cha, M.S. Kim, Photodissociation at 193 nm of some singly protonated peptides and proteins with m/z 2000-9000 using a tandem time-of-flight mass spectrometer equipped with a second source for delayed extraction/post-acceleration of product ions, Rapid Commun. Mass Spectrom. 21 (2007) 359–368. doi:10.1002/rcm.2855.

80 S.M. Greer, J.R. Cannon, J.S. Brodbelt, Improvement of Shotgun Proteomics in the Negative Mode by Carbamylation of Peptides and Ultraviolet Photodissociation Mass Spectrometry, Analytical Chemistry. 86 (2014) 12285–12290. doi:10.1021/ac5035314.

81 J.P. O'Brien, W. Li, Y. Zhang, J.S. Brodbelt, Characterization of Native Protein Complexes Using Ultraviolet Photodissociation Mass Spectrometry, Journal of the American Chemical Society. 136 (2014) 12920–12928. doi:10.1021/ja505217w.

82 M.R. Robinson, K.L. Moore, J.S. Brodbelt, Direct Identification of Tyrosine Sulfation by using Ultraviolet Photodissociation Mass Spectrometry, Journal of The American Society for Mass Spectrometry. 25 (2014) 1461–1471. doi:10.1007/s13361-014-0910-3.

83 R.S. Johnson, S.A. Martin, K. Biemann, Collision-induced fragmentation of (M + H)+ ions of peptides. Side chain specific sequence ions, International Journal of Mass Spectrometry and Ion Processes. 86 (1988) 137–154. doi:10.1016/0168-1176(88)80060-0.

84 J.A. Madsen, J.S. Brodbelt, Comparison of infrared multiphoton dissociation and collision-induced dissociation of supercharged peptides in ion traps, J. Am. Soc. Mass Spectrom. 20 (2009) 349–358. doi:10.1016/j.jasms.2008.10.018.

85 S.H. Yoon, Y.J. Chung, M.S. Kim, Time-resolved photodissociation of singly protonated peptides with an arginine at the N-terminus: A statistical interpretation, Journal of the American Society for Mass Spectrometry. 19 (2008) 645–655. doi:10.1016/j.jasms.2008.02.003.